Arch Comput Methods Eng (2010) 17: 351–372
DOI 10.1007/s11831-010-9053-2

ORIGINAL PAPER

Proper Generalized Decomposition for Multiscale and Multiphysics Problems

David Néron · Pierre Ladevèze

Received: 15 March 2010 / Accepted: 15 March 2010 / Published online: 27 October 2010

Abstract This paper is a review of the developments of the Proper Generalized Decomposition (PGD) method for the resolution, using the multiscale/multiphysics LATIN method, of the nonlinear, time-dependent problems ((visco)plasticity, damage, ...) encountered in computational mechanics. PGD leads to considerable savings in terms of computing time and storage, and makes engineering problems which would otherwise be completely out of range of industrial codes accessible.

1 Introduction

Numerical simulation is playing an increasingly important role in disciplines related to science and engineering, and one can observe a growing interest in methods which enable an accurate prediction of the behavior of a system or structure. One of the most visible signs is the willingness of the world's main industrial actors to turn to "Virtual Testing". The objective of simulation is not to replace experimental tests altogether, but to reduce their extent by choosing them more appropriately and preparing them better. In order to increase one's confidence in numerical results, it is often necessary to take into account as many of the interacting physical systems as possible and describe them on scales which can be very refined. Thus, one must be capable of dealing with problems in which several very different scales can be identified and in which different physics can be coupled. These are referred to as "multiscale" and "multiphysics" problems.

The use of standard resolution techniques based on the finite element method can be considered in order to solve such problems provided that today's computational means, particularly parallel computing, are used to their fullest extent. Unfortunately, in some cases, the number of degrees of freedom leads to systems so large that direct techniques are inapplicable and it is necessary to introduce new methods. The method which will be described in detail here is the LArge Time INcrement (LATIN) strategy [51]), with particular emphasis on the use of what is now called Proper Generalized Decomposition (PGD) to reduce computation costs. The LATIN technique, which was originally introduced under the name "Radial Approximation" in [47] in the context of evolution problems, consists in seeking an approximate solution $f(t, \underline{M})$ of a problem defined over a time-space domain using a "finite sum decomposition":

$$f(t, \underline{M}) \approx \breve{f}_p(t, \underline{M}) = \sum_{i=1}^{p} \lambda_i(t) \Lambda_i(\underline{M}) \tag{1}$$

then constructing the best decomposition of the previous form automatically. More recently, PGD was extended to other contexts, such as the resolution of what one calls "multidimensional" problems, in which a very large number of variables can interact [2, 3, 12], or the resolution of stochastic problems (in which case one talks about "Generalized Spectral Decomposition") [70, 71]. Within the framework of the LATIN method, the PGD technique has given rise to a large number of works since its introduction. Those which have been included in this review paper are the works, now considered to be mature, which concern the treatment of multiscale problems in space and time and the treatment of multiphysics problems.

D. Néron (✉) · P. Ladevèze
LMT-Cachan, ENS Cachan/CNRS/UPMC/PRES UniverSud, Paris, France
e-mail: neron@lmt.ens-cachan.fr

P. Ladevèze
e-mail: ladeveze@lmt.ens-cachan.fr

Generally speaking, representations of the "finite sum decomposition" type are clearly related to the definition of the Proper Orthogonal Decomposition (POD: see, e.g., [11]) of function f by saying that $\check{f}_p$ minimizes the distance to f in the sense of a certain norm. The POD technique, also known as Karhunen-Loève decomposition [43], Singular Value Decomposition [32] (in the discrete case) or Principal Component Decomposition [42], was the source of a great many model reduction techniques, known as *a posteriori* techniques, particularly for the resolution of problems defined over a very large time interval or for series of "similar" problems (see, e.g., [38, 45, 60, 61]). These techniques are based on the resolution, in what is called a "learning" phase, of a related problem which is less costly than the original problem, whose solution is decomposed using POD. Then, the initial model is reduced through its projection over the resulting basis, leading to an inexpensive resolution. Thus, the quality of the solution obtained is highly dependent on the proper choice of the related problem, which is one of the main drawbacks of these methods, even though techniques have been proposed to enrich the basis automatically if it is found to be insufficient to represent the solution [75, 76]. Conversely, PGD is an *a priori* model reduction technique because it consists in generating, directly and automatically, the best decomposition of type (1) for the problem one seeks to solve without relying on particular bases of functions of time or functions of space and without attempting to orthogonalize it.

In this paper, we synthesize the works presented in [52, 55, 56, 72] in order to deal with multiscale problems. These works consist in partitioning the space-time domain: the structure is defined as an assembly of substructures and interfaces, each with its own variables and its own equations. The time interval is divided into subintervals, using the discontinuous Galerkin method to handle possible discontinuities. Two scales (the microscale and the macroscale) are introduced in order to define the interface variables. The connection between the macroscale and the microscale takes place only at the interfaces. Each quantity of interest is considered to be the sum of a macro quantity and a micro quantity, the macro quantities being viewed as "mean values" in time and in space while the associated micro quantities are the complementary parts. Then, the LATIN method is used to solve the problem incrementally. At each iteration, one must solve a macro problem, defined over the entire structure and the entire time interval, along with a family of independent linear problems, each concerning a particular substructure and its boundary. The latter problems are called "micro" problems in contrast with the "macro" problem which corresponds to the entire structure homogenized in both time and space. In these works, the PGD technique was used to drastically reduce the cost of the resolution of the numerous micro problems (whose sizes can be very large) within the cells or substructures. As the iterative process goes on, the functions of the space variables constructed with the PGD technique form a consistent basis which can be reused for successive iterations.

Concerning multiphysics problems, the works described here come from [20, 68]. In these papers, the feasibility of the method was tested through the simulation of the transient saturated poroelastic evolution of a medium whose physics involves the fluid phase in connected cavities and the solid phase as the skeleton of the porous medium; both entities were homogenized, leading to a highly coupled multifield problem. In such a problem, the unknowns associated with each physics are assumed to be defined over the whole time-space domain and the coupling is defined through the constitutive relations, which implies that the coupled problem to be solved is defined over the whole time-space domain. The strategy which was used consists in generalizing the concept of a geometric interface between substructures to that of an interface among physics [20]. This interface is defined over the whole time-space domain and its behavior consists in the verification of the constitutive relations which couple the physics. Then, the remaining compatibility and equilibrium equations are global equations defined over the whole time-space domain, but they are uncoupled with respect to the physics. The LATIN method is used to generate iteratively a solution which verifies both the global, single-physics equations and the local, coupled equations which constitute the interfaces among the physics. The number of fields involved and, therefore, the number of single-physics global problems to be solved over the whole time interval can be very large. Again, the PGD technique was used to achieve a drastic reduction in the cost of constructing and storing these fields.

The paper is structured as follows: in Sect. 2, we present an overview of Proper Generalized Decomposition, with particular emphasis on how a problem defined over the space-time domain can be rewritten in the form of a minimization problem and how this minimization problem can be handled; in Sect. 3, we introduce the LATIN method as a solver for a nonlinear evolution problem; in Sect. 4, we show how PGD enables a reduction in computation cost; in Sect. 5, we illustrate the use of that method for the resolution of a viscoelastic problem involving contact surfaces with friction; finally, in Sect. 6, we present the LATIN method for multiphysics problems in the particular case of a porous medium.

2 The Proper Generalized Decomposition Technique

2.1 Justification for Using Separated Time and Space Representations

In this section, we follow [51] and consider a time-space domain $I \times \Omega$ where $I = [0, T]$ and $\Omega \subset \mathbb{R}^d$. With f being

a known scalar function defined over $I \times \Omega$, let us study the "best" pth-order time-space approximation of function f:

$$\check{f}_p(t, \underline{M}) = \sum_{i=1}^{p} \lambda_i(t) \Lambda_i(\underline{M}) \tag{2}$$

λ_i and Λ_i constitute reduced bases of the spaces of the time and space functions respectively. The idea of Proper Orthogonal Decomposition (POD), also known as Principal Component Decomposition [42] or, in the finite-dimensional case, Singular Value Decomposition [32], is to define the approximation $\check{f}_p$ as that which minimizes the distance to the initial function f with respect to a particular norm $\|\cdot\|_{I\times\Omega}$:

$$\check{f}_p = \sum_{i=1}^{p} \lambda_i \Lambda_i = \arg\min_{\lambda_i, \Lambda_i} \left\| f - \sum_{i=1}^{p} \lambda_i \Lambda_i \right\|_{I\times\Omega}^2 \tag{3}$$

Classically, the norm chosen is that which is associated with the scalar product:

$$\langle f, g \rangle_{I\times\Omega} = \int_{I\times\Omega} fg \, d\Omega dt \tag{4}$$

Then, if one introduces the following scalar products:

$$\langle f, g \rangle_I = \int_I fg \, dt \quad \text{and} \quad \langle f, g \rangle_\Omega = \int_\Omega fg \, d\Omega \tag{5}$$

one can prove that (3) is an eigenvalue problem whose eigenfunctions are the time functions λ_i. This problem can be rewritten as the stationarity of the Rayleigh quotient:

$$R(\lambda) = \frac{\|\langle f, \lambda \rangle_I\|_\Omega^2}{\|\lambda\|_I^2} \tag{6}$$

Under classical regularity assumptions on f, the eigenvalue problem has a countable sequence of eigensolutions $(\alpha_i^{-1}, \lambda_i)$, with the eigenvalues α_i^{-1} being positive and the eigenfunctions λ_i orthogonal.

Once the time functions λ_i have been determined, the corresponding space functions Λ_i are:

$$\Lambda_i = \frac{\langle f, \lambda_i \rangle_I}{\|\lambda_i\|_I^2} \tag{7}$$

The following convergence property is verified:

$$\|f - \check{f}_p\|_{I\times\Omega} \underset{p\to+\infty}{\longrightarrow} 0 \tag{8}$$

and a simple measure of the relative error is:

$$\eta_p = \frac{\|f - \check{f}_p\|_{I\times\Omega}}{\|\frac{1}{2}(f + \check{f}_p)\|_{I\times\Omega}} \tag{9}$$

To illustrate the relevance of separated time and space representations, let us consider the case of a randomly-obtained irregular function f defined over a time-space domain $I \times [0, L]$ in which space is one-dimensional. Figure 1 shows function f along with its first-, second- and third-order approximations. The relative error achieved with only 3 radial functions was less than 1%, which gives an idea of the remarkable accuracy achievable with the proposed time-space approximation.

2.2 *A Posteriori* and *A Priori* Model Reduction

The previous decomposition can be performed when function f is known. This type of technique is commonly used in the context of data analysis when the objective is a low-dimensional approximate description of a high-dimensional process (see [11] for a discussion of some applications in the context of dynamic systems), as well as in image processing applications when the objective is to extract the most relevant part of an image in order to compress the data.

When function f is unknown (because it is the solution of a complex problem which must be solved), the separated representation technique can also be used to reduce the computational cost of the simulation. The most popular technique, known as the *a posteriori* reduction method (see, e.g., [38, 45, 60, 61]), is based on the principle of solving a related problem which is much simpler than the original problem (typically, the same as the original problem, but over a very short time interval or, conversely, the problem defined over the whole time interval, but with a very coarse time discretization or the resolution for a given set of parameters if the objective is to carry out a sensitivity analysis). Then, the solution obtained in this "learning" phase (called a "snapshot") is decomposed through POD, and the resulting reduced basis (e.g. the truncated basis of the space functions) is used to project the equations of the initial problem. The resolution of the problem thus reduced is much less costly than that of the initial problem and the quality of the result can be evaluated *a posteriori*, for example by measuring a residual error. Of course, the quality of that solution is highly dependent on the choice of the related problem used in the learning phase. Indeed, the basis resulting from the decomposition of the snapshot can be insufficient to provide a refined representation of the still unknown solution of the initial problem, and it is necessary to reach a compromise between that and a learning phase which would bring in a wealth of information, but would be costly in computing time. Strategies were proposed in [75, 76] to overcome this difficulty by controlling the error in the solution and enriching the initial basis in the process. However, difficulties have been observed in some cases (including particularly the wave equation) where the enrichment, based on the use of Krylov subspaces, was not optimal.

Directly opposed to these *a posteriori* techniques are *a priori* model reduction techniques, whose objective is to generate the best approximation of the solution of the problem in separated form directly. These methods, based on

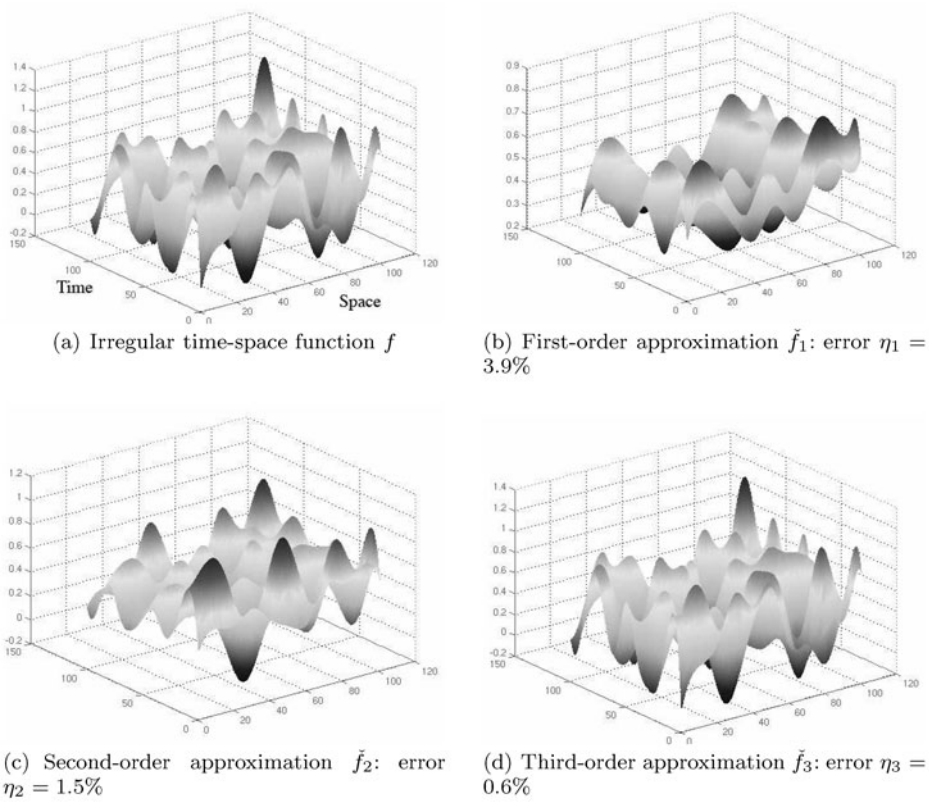

(a) Irregular time-space function f

(b) First-order approximation $\check{f}_1$: error $\eta_1 = 3.9\%$

(c) Second-order approximation $\check{f}_2$: error $\eta_2 = 1.5\%$

(d) Third-order approximation $\check{f}_3$: error $\eta_3 = 0.6\%$

Fig. 1 Time-space approximations of an irregular function f

what was recently named Proper Generalized Decomposition (PGD), require the implementation of algorithms which are quite unlike the usual incremental techniques. Among the works dealing with PGD, one can mention the resolution of what one calls multidimensional problems, in which a very large number of variables can interact [3, 12], or the resolution of stochastic problems [70, 71] (in which case one uses the term "Generalized Spectral Decomposition"). In the following sections, we will study the use of the LATIN method for the resolution of a nonlinear evolution problem and we will show how PGD can lead to a reduction in the computation cost.

3 The LATIN Method as a Nonlinear Solver

3.1 The Reference Problem

In order to illustrate the method, let us consider the case of the quasi-static, isothermal evolution of a structure defined over the time-space domain $I \times \Omega$, where $I = [0, T]$ and $\Omega \subset \mathbb{R}^d$. Under the assumption of small perturbations, the state of the structure is defined by: $\boldsymbol{\varepsilon}_p$, the inelastic part of the strain field $\boldsymbol{\varepsilon}$ corresponding to the displacement field $\underline{U}$, which uncouples into an elastic part $\boldsymbol{\varepsilon}_e$ and an inelastic part $\boldsymbol{\varepsilon}_p = \boldsymbol{\varepsilon} - \boldsymbol{\varepsilon}_e$; $\mathbf{X}$, the remaining internal variables; $\boldsymbol{\sigma}$, the Cauchy stress field; and $\mathbf{Y}$, the set of variables conjugate of $\mathbf{X}$. All these quantities are defined over the time-space domain $I \times \Omega$ and are assumed to be sufficiently regular. Introducing the following notations for the primal and dual fields:

$$\mathbf{u} = \begin{bmatrix} U \\ 0 \end{bmatrix}, \qquad \mathbf{e}_p = \begin{bmatrix} \boldsymbol{\varepsilon}_p \\ -\mathbf{X} \end{bmatrix}, \qquad \mathbf{e} = \begin{bmatrix} \boldsymbol{\varepsilon} \\ 0 \end{bmatrix}, \qquad \mathbf{e}_e = \begin{bmatrix} \boldsymbol{\varepsilon}_e \\ \mathbf{X} \end{bmatrix},$$

$$\text{so that} \quad \mathbf{e}_p = \mathbf{e} - \mathbf{e}_e \quad \text{and} \quad \mathbf{f} = \begin{bmatrix} \boldsymbol{\sigma} \\ \mathbf{Y} \end{bmatrix} \tag{10}$$

the mechanical dissipation rate for the entire structure Ω is:

$$\int_\Omega (\dot{\boldsymbol{\varepsilon}}_p : \boldsymbol{\sigma} - \dot{\mathbf{X}} \cdot \mathbf{Y}) d\Omega = \int_\Omega (\dot{\mathbf{e}}_p \circ \mathbf{f}) d\Omega \tag{11}$$

where $\cdot$ denotes the contraction associated with the tensorial nature of $\mathbf{X}$ and $\mathbf{Y}$, and $\circ$ denotes the corresponding operator. Let us introduce the bilinear "dissipation" form:

$$\langle \mathbf{s}, \mathbf{s}' \rangle = \int_{I \times \Omega} \left(1 - \frac{t}{T}\right) (\dot{\mathbf{e}}_p \circ \mathbf{f}' + \dot{\mathbf{e}}'_p \circ \mathbf{f}) \, d\Omega dt \tag{12}$$

along with $\mathbf{E}$ and $\mathbf{F}$, the spaces of the fields $\dot{\mathbf{e}}_p$ and $\mathbf{f}$ which are compatible with (12) (using $\dot{\square}$ to designate the time derivative). These spaces enable us to define $\mathbf{S} = \mathbf{E} \times \mathbf{F}$, the space in which the state $\mathbf{s} = (\dot{\mathbf{e}}_p, \mathbf{f})$ of the structure is being sought.

A normal formulation with internal state variables is used to represent the behavior of the material. The *state law* is

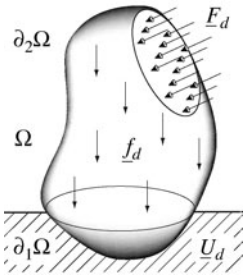

Fig. 2 The reference problem and boundary conditions

assumed to lead to:

$$\mathbf{f} = \mathbf{A}\mathbf{e}_{\mathrm{e}} \quad \text{with } \mathbf{A} = \begin{bmatrix} \mathbf{K} & 0 \\ 0 & \mathbf{\Lambda} \end{bmatrix} \tag{13}$$

where Hooke's tensor $\mathbf{K}$ and the constant, symmetric and positive definite tensor $\mathbf{\Lambda}$ are characteristics of the material and, therefore, operator $\mathbf{A}$ is constant, symmetric and positive definite. The *evolution law*, which can be nonlinear, is assumed to be given by the positive differential operator $\mathbf{B}$ such that:

$$\dot{\mathbf{e}}_{\mathrm{p}} = \mathbf{B}(\mathbf{f}) \tag{14}$$

Let us note that such a behavior formulation is available for most material models. For a detailed description of operators $\mathbf{A}$ and $\mathbf{B}$ in the cases of viscoelastic or viscoplastic materials, the reader can refer to [51].

In this reference problem, the structure is subjected to prescribed body forces $\underline{f}_d$, traction forces $\underline{F}_d$ over a part $\partial_2\Omega$ of the boundary, and displacements $\underline{U}_d$ over the complementary part $\partial_1\Omega$ (see Fig. 2). For the sake of simplicity, the displacement $\underline{U}$ alone is assumed to have a nonzero initial value denoted $\underline{U}_0$. In order to formulate the reference problem, let us introduce the following functional subspaces of $\mathbf{S}$ (where $\square^\star$ denotes vector spaces associated with affine spaces):

- *the space* $\boldsymbol{\mathcal{U}}$ *of the kinematically admissible fields* $\mathbf{u}$ whose displacement $\underline{U}$ is equal to the prescribed displacement $\underline{U}_d$ over $\partial_1\Omega$ and verifies the initial conditions $\underline{U}_0$: $\underline{U}_{|\partial_1\Omega} = \underline{U}_d$ and $\underline{U}_{|t=0} = \underline{U}_0$.
- *the space* $\boldsymbol{\mathcal{F}}$ *of the statically admissible fields* $\mathbf{f}$ whose stress field $\boldsymbol{\sigma}$ is in equilibrium with the prescribed external forces $\underline{F}_d$ over $\partial_2\Omega$ and verifies the momentum conservation equation:

$$\forall \mathbf{u}^\star \in \boldsymbol{\mathcal{U}}^\star, \quad -\int_{I\times\Omega} \mathbf{f}\circ\mathbf{e}(\dot{\underline{U}}^\star)\, d\Omega dt + \int_{I\times\Omega} \underline{f}_d \cdot \dot{\underline{U}}^\star\, d\Omega dt + \int_{I\times\partial_2\Omega} \underline{F}_d \cdot \dot{\underline{U}}^\star\, dS dt = 0 \tag{15}$$

- *the space* $\boldsymbol{\mathcal{E}}$ *of the kinematically admissible fields* $\dot{\mathbf{e}}$ whose strain field $\boldsymbol{\varepsilon}$ derives from a displacement field $\underline{U}$ belonging to $\boldsymbol{\mathcal{U}}$:

$$\forall \mathbf{f}^\star \in \boldsymbol{\mathcal{F}}^\star, \quad -\int_{I\times\Omega} \mathbf{f}^\star\circ\dot{\mathbf{e}}\, d\Omega dt + \int_{I\times\partial_1\Omega} \boldsymbol{\sigma}^\star \underline{n}\cdot\dot{\underline{U}}_d\, dS dt = 0 \tag{16}$$

- *the space* $\mathbf{A_d}$ *of the admissible fields* $\mathbf{s}$ in which $\mathbf{f}$ is statically admissible, $\mathbf{f}$ and $\dot{\mathbf{e}}_{\mathrm{p}}$ verify the state law (13), and the corresponding $\dot{\mathbf{e}}$ is kinematically admissible:

$$\mathbf{f} \in \boldsymbol{\mathcal{F}}, \quad (\mathbf{A}^{-1}\dot{\mathbf{f}} + \dot{\mathbf{e}}_{\mathrm{p}}) \in \boldsymbol{\mathcal{E}} \tag{17}$$

- *the space* $\mathbf{\Gamma}$ *of the fields* $\mathbf{s}$ in which $\mathbf{f}$ and $\dot{\mathbf{e}}_{\mathrm{p}}$ verify the evolution law (14):

$$\dot{\mathbf{e}}_{\mathrm{p}} = \mathbf{B}(\mathbf{f}) \tag{18}$$

Obviously, the solution $\mathbf{s_{ref}}$ of the problem over the time-space domain $I\times\Omega$ can be viewed as the intersection of $\mathbf{A_d}$ and $\mathbf{\Gamma}$. Then, the reference problem becomes:

$$\text{Find } \mathbf{s_{ref}} \in \mathbf{A_d} \cap \mathbf{\Gamma} \tag{19}$$

It is important to note that $\mathbf{A_d}$ is a set of solutions of global linear equations, while $\mathbf{\Gamma}$ is a set of solutions of (possibly) nonlinear equations which are local in time and in space.

Nearly all the methods available in mechanics for the resolution of nonlinear evolution problems such as (19) are incremental methods. The time interval $I = [0, T]$ being considered is decomposed into a series of small intervals. Assuming that the history of the different quantities until the current time t is known, the objective is to study the new interval $[t, t+\Delta t]$, where Δt denotes the increment. For example, the assumption that the evolution over $[t, t+\Delta t]$ is linear, *i.e.* that the history depends only on the values at time $t+\Delta t$, leads to a nonlinear problem which does not involve time and which can be solved by a Newton-type method. Roughly speaking, this type of method requires the resolution of about $n_I \times n_N$ spatial problems for the Newton scheme to converge (n_I being the number of time intervals in I and n_N the number of subiterations, which is assumed to be constant).

The LATIN method, which will be described next, relies on a different scheme which takes advantage of the favorable properties of the equations (linearity of $\mathbf{A_d}$ and locality of $\mathbf{\Gamma}$) while avoiding the simultaneous treatment of their difficult aspects (the globality of $\mathbf{A_d}$ and the nonlinearity of $\mathbf{\Gamma}$).

3.2 The LATIN Method as a Solver

Let us apply the LATIN method to the formulation of the problem to be solved presented previously (19). The LATIN method is a general, mechanics-based computational strategy for the resolution of time-dependent nonlinear problems

Fig. 3 The local stage and the linear stage of the LATIN method at iteration $n+1$

$$\cdots \longrightarrow \mathbf{s}_n \in \mathbf{A_d} \xrightarrow{\text{local stage}} \hat{\mathbf{s}}_{n+1/2} \in \boldsymbol{\Gamma} \xrightarrow{\text{linear stage}} \mathbf{s}_{n+1} \in \mathbf{A_d} \longrightarrow \hat{\mathbf{s}}_{n+3/2} \longrightarrow \cdots$$

Iteration $n+1$

which operates over the entire time-space domain [48, 51]. The solution of the problem is obtained through an iterative scheme. An iteration consists of two stages, called the "local stage" and the "linear stage". As shown in Fig. 3, these stages consist in building fields of $\boldsymbol{\Gamma}$ and $\mathbf{A_d}$ alternatively. Under conditions which will described later, this iterative process converges toward the solution $\mathbf{s_{ref}}$ of the problem. The two stages of the method will be described in detail in the following sections.

It is important to note that at any given iteration $n+1$ of the method two approximate solutions ($\hat{\mathbf{s}}_{n+1/2} \in \boldsymbol{\Gamma}$ and $\mathbf{s}_{n+1} \in \mathbf{A_d}$) are known over the entire time-space domain $I \times \Omega$. In that sense, the LATIN method is considered to be "nonincremental", contrary to incremental methods, in which an approximate solution is achieved only once the algorithm has been carried out through the entire time interval. Figure 4 illustrates the LATIN algorithm by showing, in the space $\mathbf{S} = \mathbf{E} \times \mathbf{F}$ in which the solution is sought, the linear space $\mathbf{A_d}$ and the nonlinear space $\boldsymbol{\Gamma}$ along with the solution $\mathbf{s_{ref}}$. It is clear that in order to complete our coverage of the problem we also need to introduce what we call the "search directions" $\mathbf{E}^+$ and $\mathbf{E}^-$. This will be done later.

3.3 The Local Stage at Iteration $n+1$

This stage consists, given $\mathbf{s}_n \in \mathbf{A_d}$, in building $\hat{\mathbf{s}}_{n+1/2} \in \boldsymbol{\Gamma}$, then using an "ascent" search direction $\mathbf{E}^+$ followed by $\hat{\mathbf{s}}_{n+1/2} - \mathbf{s}_n = \delta\mathbf{s}$ (see Fig. 4). This search direction is defined by:

$$\mathbf{E}^+ = \{\delta\mathbf{s} = (\delta\dot{\mathbf{e}}_p, \delta\mathbf{f}) \mid \delta\dot{\mathbf{e}}_p + \mathbf{H}^+\delta\mathbf{f} = 0\} \tag{20}$$

where $\mathbf{H}^+$ is a symmetric, positive definite operator which is a parameter of the method. One can easily show that seeking $\hat{\mathbf{s}}_{n+1/2} = (\hat{\dot{\mathbf{e}}}_p, \hat{\mathbf{f}})$ common to $\boldsymbol{\Gamma}$ and $\mathbf{E}^+$ leads to the resolution of a set of nonlinear problems:

$$\mathbf{B}(\hat{\mathbf{f}}) + \mathbf{H}^+\hat{\mathbf{f}} = \mathbf{a}_n \tag{21}$$

whose right-hand sides $\mathbf{a}_n = \dot{\mathbf{e}}_{pn} + \mathbf{H}^+\mathbf{f}_n$ are known at this stage, and which are *local in the space variable*. Therefore, these problems lend themselves to the highest degree of parallelism. This property justifies the term "local" used to designate this stage. Once problems (21) have been solved, one determines $\hat{\dot{\mathbf{e}}}_p$ using search direction $\mathbf{E}^+$, *i.e.* by setting $\hat{\dot{\mathbf{e}}}_p = \mathbf{a}_n - \mathbf{H}^+\mathbf{f}$.

3.4 The Linear Stage at Iteration $n+1$

This stage consists, given $\hat{\mathbf{s}}_{n+1/2} \in \boldsymbol{\Gamma}$, in building $\mathbf{s}_{n+1} \in \mathbf{A_d}$, then using a "descent" search direction $\mathbf{E}^-$ followed by

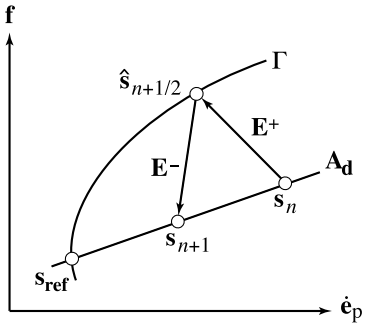

Fig. 4 An iteration of the LATIN method

$\mathbf{s}_{n+1} - \hat{\mathbf{s}}_{n+1/2} = \delta\mathbf{s}$ (see Fig. 4). This search direction is defined by:

$$\mathbf{E}^- = \{\delta\mathbf{s} = (\delta\dot{\mathbf{e}}_p, \delta\mathbf{f}) \mid \delta\dot{\mathbf{e}}_p - \mathbf{H}^-\delta\mathbf{f} = 0\} \tag{22}$$

where $\mathbf{H}^-$ is a symmetric, positive definite operator which is a parameter of the method. One can show that seeking $\mathbf{s}_{n+1} = (\dot{\mathbf{e}}_p, \mathbf{f})$ common to $\mathbf{A_d}$ and $\mathbf{E}^-$ leads to the resolution of a global problem in space:

$$\forall \mathbf{f}^\star \in \mathcal{F}^\star, \quad \int_{I\times\Omega} \mathbf{f}^\star \circ (\mathbf{A}^{-1}\dot{\mathbf{f}} + \mathbf{H}^-\mathbf{f})\, d\Omega dt$$
$$= \int_{I\times\Omega} \mathbf{f}^\star \circ \hat{\mathbf{a}}\, d\Omega dt + \int_{I\times\partial_1\Omega} \boldsymbol{\sigma}^\star \underline{n} \cdot \underline{\dot{U}}_d\, dS dt = 0 \tag{23}$$

whose right-hand side $\hat{\mathbf{a}} = \hat{\dot{\mathbf{e}}}_p - \mathbf{H}^-\hat{\mathbf{f}}$ is known at this stage and where $\underline{U}_d$ is a prescribed boundary condition. This problem is *linear* (and, therefore, this stage is called the "linear" stage), but it depends on time. Its treatment will be discussed in Sect. 4. Once problem (23) has been solved, one determines $\dot{\mathbf{e}}_p$ using search direction $\mathbf{E}^-$, *i.e.* by setting $\dot{\mathbf{e}}_p = \hat{\mathbf{a}} - \mathbf{H}^-\mathbf{f}$.

3.5 Convergence Properties and Criterion

If $\mathbf{B}$ is monotonic, using the fact that $\mathbf{A}$ is symmetric and positive definite, one can derive the following anti-monotony and monotony properties:

$$\begin{aligned} &\forall (\mathbf{s}, \mathbf{s}') \in \mathbf{A_d}^2, \quad \langle \mathbf{s} - \mathbf{s}', \mathbf{s} - \mathbf{s}' \rangle \le 0 \\ &\forall (\mathbf{s}, \mathbf{s}') \in \boldsymbol{\Gamma}^2, \quad \langle \mathbf{s} - \mathbf{s}', \mathbf{s} - \mathbf{s}' \rangle \ge 0 \end{aligned} \tag{24}$$

The choice of parameters $\mathbf{H}^+$ and $\mathbf{H}^-$ influences only the convergence of the algorithm, but does not affect the solution. In practice, these parameters are chosen as $\mathbf{H}^+ = \mathbf{H}^- = \mathbf{H}$, where $\mathbf{H}$ is a symmetric, positive definite operator which

can vary during the iterative process. In that case, following the proof given in [51] based on the anti-monotony and monotony properties (24), one can prove that the quantity $\frac{1}{2}(\mathbf{s}_{n+1} + \mathbf{s}_n)$ converges toward $\mathbf{s_{ref}}$, the solution of Problem (19). If the behavior is linear, one can choose, for example, $\mathbf{H} = \mathbf{B}$. Other possible choices, especially in the nonlinear case, are discussed in [51].

In order to ensure the convergence of $\mathbf{s}_n$ and, more generally, to ensure convergence for many types of material behavior, a relaxation technique may be required. Renaming the quantity previously denoted $\mathbf{s}_{n+1}$ as $\bar{\mathbf{s}}_{n+1}$, we redefine the approximate solution $\mathbf{s}_{n+1}$ generated by linear stage $n+1$ as:

$$\mathbf{s}_{n+1} = \mu\bar{\mathbf{s}}_{n+1} + (1-\mu)\mathbf{s}_n \tag{25}$$

where μ is a relaxation parameter usually chosen to be equal to 0.8.

Since the reference solution $\mathbf{s_{ref}}$ is the intersection of $\boldsymbol{\Gamma}$ and $\mathbf{A_d}$, the distance between $\hat{\mathbf{s}}_{n+1/2}$ and $\mathbf{s}_n$ is a good error indicator for assessing the convergence of the algorithm. The simplest measure of that distance is:

$$\eta = \frac{\|\hat{\mathbf{s}}_{n+1/2} - \mathbf{s}_n\|}{\frac{1}{2}\|\hat{\mathbf{s}}_{n+1/2} + \mathbf{s}_n\|} \tag{26}$$

with:

$$\|\mathbf{s}\|^2 = \frac{1}{2}\int_{I\times\Omega} (\dot{\mathbf{e}}_\mathrm{p} \circ \mathbf{H}^{-1}\dot{\mathbf{e}}_\mathrm{p} + \mathbf{f} \circ \mathbf{H}\mathbf{f})\, d\Omega dt \tag{27}$$

4 The LATIN Method and Proper Generalized Decomposition

4.1 Using Proper Generalized Decomposition

Problem (23) is solved using the Proper Generalized Decomposition method, which was first introduced in [47] under the name "radial approximation" (see also [49, 51]). In order to do that, the linear stage at Iteration $n+1$ is rewritten as a corrective increment $\Delta\mathbf{s}$ to the previous approximation $\mathbf{s}_n$, so that the quantity being sought is no longer $\mathbf{s}_{n+1} \in \mathbf{A_d}$, but $\Delta\mathbf{s}$ such that $\mathbf{s}_{n+1} = (\dot{\mathbf{e}}_\mathrm{p}, \mathbf{f}) = \mathbf{s}_n + \Delta\mathbf{s}$.

If the initial solution $\mathbf{s}_0$ (e.g. the solution of a linear elastic calculation) belongs to $\mathbf{A_d}$, all the corrective increments $\Delta\mathbf{s} = (\Delta\dot{\mathbf{e}}_\mathrm{p}, \Delta\mathbf{f})$ are sought in $\mathbf{A}_\mathbf{d}^\star$, the space which corresponds to $\mathbf{A_d}$ with homogeneous conditions. With the choice $\mathbf{H}^- = \mathbf{H}$ mentioned previously, where $\mathbf{H}$ is a symmetric, positive definite operator, the search direction $\mathbf{E}^-$ defined by (22) becomes:

$$\Delta\dot{\mathbf{e}}_\mathrm{p} - \mathbf{H}\Delta\mathbf{f} - \Delta\hat{\mathbf{a}} = 0 \tag{28}$$

where $\Delta\hat{\mathbf{a}} = (\hat{\dot{\mathbf{e}}}_\mathrm{p} - \dot{\mathbf{e}}_{\mathrm{p}n}) - \mathbf{H}(\hat{\mathbf{f}} - \mathbf{f}_n)$, which is known at this stage, is rewritten as the minimization of a global constitutive relation error in $\mathbf{A}_\mathbf{d}^\star$:

$$\Delta\mathbf{s} = \mathrm{Arg}\min_{\Delta\mathbf{s}\in\mathbf{A}_\mathbf{d}^\star} e_{CR}^2(\Delta\mathbf{s}) = \|\Delta\dot{\mathbf{e}}_\mathrm{p} - \mathbf{H}\Delta\mathbf{f} - \Delta\hat{\mathbf{a}}\|_\mathbf{M}^2 \tag{29}$$

This expression introduces the norm:

$$\|\square\|_\mathbf{M}^2 = \int_{I\times\Omega} \square \circ \mathbf{M}\square\, d\Omega dt \tag{30}$$

where $\mathbf{M}$ a symmetric, positive definite operator usually chosen to be equal to $\mathbf{M} = (1 - \frac{t}{T})\mathbf{H}$. The new formulation (29) is equivalent to the initial problem (23) provided no approximation is introduced in seeking the corrective increment $\Delta\mathbf{s} = (\Delta\dot{\mathbf{e}}_\mathrm{p}, \Delta\mathbf{f})$.

Now, we propose to approximate the corrective increment $\Delta\mathbf{s}$ using a separated representation $\Delta\check{\mathbf{s}}$. The fields are approximated by:

$$\begin{aligned}
\Delta\dot{\mathbf{e}}_\mathrm{p}(t, \underline{M}) &\approx \Delta\check{\dot{\mathbf{e}}}_\mathrm{p}(t, \underline{M}) = \dot{a}(t)\mathbf{E}_\mathrm{p}(\underline{M}) \\
\Delta\mathbf{f}(t, \underline{M}) &\approx \Delta\check{\mathbf{f}}(t, \underline{M}) = b(t)\mathbf{F}(\underline{M}) \\
\Delta\dot{\mathbf{e}}(t, \underline{M}) &\approx \Delta\check{\dot{\mathbf{e}}}(t, \underline{M}) = \dot{c}(t)\mathbf{E}(\underline{M})
\end{aligned} \tag{31}$$

where, in order to simplify the presentation, only one pair is used for each field. (The use of more than one pair would not introduce any difficulty.)

These three corrective increments are not independent of one another because $\Delta\check{\mathbf{s}}$ is sought in $\mathbf{A}_\mathbf{d}^\star$, which expresses the fact that $\Delta\check{\mathbf{f}} \in \boldsymbol{\mathcal{F}}$ and $\Delta\check{\dot{\mathbf{e}}} = \mathbf{A}^{-1}\Delta\check{\mathbf{f}} + \Delta\check{\dot{\mathbf{e}}}_\mathrm{p} \in \boldsymbol{\mathcal{E}}$. These two conditions lead to:

$$\forall\dot{\mathbf{e}}^\star \in \boldsymbol{\mathcal{E}}^\star, \quad \int_{I\times\Omega} \dot{\mathbf{e}}^\star \circ \mathbf{A}\Delta\check{\dot{\mathbf{e}}}\, d\Omega dt = \int_{I\times\Omega} \dot{\mathbf{e}}^\star \circ \mathbf{A}\Delta\check{\dot{\mathbf{e}}}_\mathrm{p}\, d\Omega dt \tag{32}$$

which shows that if a and $\mathbf{E}_\mathrm{p}$ are known one has $c = a$ and then $\mathbf{E}$ is obtained by solving the following problem:

$$\forall\mathbf{E}^\star \in \boldsymbol{\mathcal{E}}^\star, \quad \int_\Omega \mathbf{E}^\star \circ \mathbf{A}(\mathbf{E} - \mathbf{E}_\mathrm{p})d\Omega = 0 \tag{33}$$

This is a classical time-independent global problem which consists in finding $\mathbf{E} = [\boldsymbol{\varepsilon}(\Delta\underline{U})\ 0]^T$ given $\Delta\underline{U} \in \boldsymbol{\mathcal{U}}^\star$ such that:

$$\forall\underline{U}^\star \in \boldsymbol{\mathcal{U}}^\star, \quad \int_\Omega \boldsymbol{\varepsilon}(\underline{U}^\star) : \mathbf{K}(\boldsymbol{\varepsilon}(\Delta\underline{U}) - \boldsymbol{\varepsilon}_\mathrm{p})d\Omega = 0 \tag{34}$$

Next, if the corrective increments $\Delta\check{\dot{\mathbf{e}}}_\mathrm{p}$ and $\Delta\check{\dot{\mathbf{e}}}$ are known, the corrective increment $\Delta\check{\mathbf{f}}$ is obtained by $b = a$ and $\mathbf{F} = \mathbf{A}(\mathbf{E} - \mathbf{E}_\mathrm{p})$. Finally, we saw that $\Delta\check{\mathbf{s}}$ is defined entirely by one's knowledge of the time function $a(t)$ and the space

function $\mathbf{E}_{\mathrm{p}}(\underline{M})$. Problem (29) can then be rewritten in terms of these unknowns:

$$\Delta\check{\mathbf{s}} = \mathrm{Arg}\min_{\Delta\check{\mathbf{s}}\in\mathbf{A}_{\mathbf{d}}^{\star}} e_{CR}^2(\Delta\check{\mathbf{s}}) = \|\dot{a}\mathbf{E}_{\mathrm{p}} - a\mathbf{HF} - \Delta\hat{\mathbf{a}}\|_{\mathbf{M}}^2 \qquad (35)$$

which is solved using the technique described below.

4.2 Generation of the PGD Corrective Terms at Iteration $n+1$

In order to solve (35), one seeks minima with respect to time (leading to a system of differential equations) and space (leading to a spatial problem) alternatively using Algorithm 1. Let us focus on Iteration $n+1$ and assume that we have at our disposal a reduced basis $(a_i, \mathbf{E}_{\mathrm{p}i})_{i=0}^{n}$ such that $\dot{\mathbf{e}}_{\mathrm{p}n} = \dot{a}_0\mathbf{E}_{\mathrm{p}0} + \sum_{i=1}^{n}\dot{a}_i\mathbf{E}_{\mathrm{p}i}$, which enables us to define $\mathbf{f}_n = b_0\mathbf{F}_0 + \sum_{i=1}^{n} a_i\mathbf{F}_i$. The initial pair $(\dot{a}_0\mathbf{E}_{\mathrm{p}0}, b_0\mathbf{F}_0)$ belongs to $\mathbf{A}_{\mathbf{d}}$ while each of the n following pairs $(\dot{a}_i\mathbf{E}_{\mathrm{p}_i}, a_i\mathbf{F}_i)$ belongs to $\mathbf{A}_{\mathbf{d}}^{\star}$. The objective is to generate a new corrective term $\dot{a}\mathbf{E}_{\mathrm{p}}$ for the primal field and derive the correction $a\mathbf{F}$ for the dual field. The two main steps of the algorithm are:

input: the previous approximation $\mathbf{e}_{\mathrm{p}_n} = a_0\mathbf{E}_{\mathrm{p}0} + \sum_{i=1}^{n} a_i\mathbf{E}_{\mathrm{p}_i}$ and the known quantities $\Delta\hat{\mathbf{a}}$

Step 1: use of the reduced basis
keeping the space functions $(\mathbf{E}_{\mathrm{p}i})_{i=1}^{n}$ fixed, one seeks the $(a_i)_{i=1}^{n}$ which minimize e_{CR}^2;

Step 2: addition of new functions
initialization: $a^0(t)$ (for example, $f(t) = \alpha t$);
for $k = 1$ **to** k_{max} **do**

- **spatial problem:** given the time function $a^k(t)$, one seeks the $\mathbf{E}_{\mathrm{p}}^k$ which minimize e_{CR}^2;
- **time problem:** given the space functions $\mathbf{E}_{\mathrm{p}}^k$, one seeks $a^k(t)$ which minimizes e_{CR}^2;
- **orthonormalization** of the space functions with respect to the previous spatial basis;

end

Algorithm 1: Iterative generation of the PGD corrective terms at Iteration $n+1$

Step 1: use of the reduced basis. This phase consists in formulating an inexpensive prediction thanks to one's knowledge of the solutions from previous iterations. This approximate solution is introduced into the constitutive relation error (35), but in this case the only unknowns are the time functions. In other words, one seeks the optimum combination of the reduced basis of space functions which minimizes the constitutive relation error e_{CR}^2. These time functions verify a system of linear differential equations in time with conditions at $t = 0$ and $t = T$, whose solution is obtained classically. This is usually a relatively small system.

Step 2: addition of new functions. With the predicted solution obtained previously, one seeks a new approximate solution. The minimization with respect to the space variables leads to the resolution of a time-independent spatial problem defined over Ω. The minimization with respect to the time variable leads to a scalar differential equation defined over I, whose resolution is quite inexpensive. Once these new space and time functions have been calculated, the space functions are orthogonalized and added to the reduced basis.

Since the construction of the space functions is by far the most expensive part of the process, it is advisable to store and reuse these functions. Thus, the space functions constructed up to Iteration n can be reused at Iteration $n+1$ and Step 1 is executed systematically only to update the corresponding time functions. Conversely, Step 2, which generates new time and space functions, can be skipped if the correction from Step 1 is sufficient. (This technique requires an *ad hoc* criterion to be set up.)

4.3 Discussion of the Computational Cost

The resolution of Problem (23) using a standard incremental technique would have required the resolution of n_I spatial problems at each iteration of the LATIN algorithm, n_I being the number of time intervals in I. Then, the generation of the final approximation of the solution $\mathbf{s}_{\mathbf{ref}}$ would have required the resolution of $n_I \times n_{iter}$ spatial problems, n_{iter} being the number of iterations of the LATIN method necessary for a given accuracy assessed by the convergence of indicator η. The latter would have been by far the costliest part of the algorithm. In that form, the LATIN method could be viewed as a Newton-type algorithm except for an inversion of the order in which the iterations corresponding to the treatment of the nonlinearity and those corresponding to the treatment of the time evolution are performed, which would result in no decrease in computation costs.

When the PGD technique is used, as can be seen in our examples, Algorithm 1 converges very quickly. Therefore, in practice, k_{max} is set to be equal to only 2 or 3. Then, the generation of the final approximation of the solution $\mathbf{s}_{\mathbf{ref}}$ requires the resolution of $k_{max} \times n_{iter}$ spatial problems, and n_{iter} (the number of iterations of the LATIN method necessary for a given accuracy assessed by the convergence of indicator η) is nearly the same as in the case of an incremental strategy. Thus, the decrease in computation cost compared to a Newton-type algorithm is obvious.

4.4 Practical Implementation in Order to Reduce Storage Requirements

Working with the PGD description alone constitutes a very convenient framework in which the storage requirement is

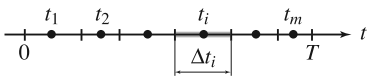

Fig. 5 The reference times in I

Fig. 6 The reference points in Ω

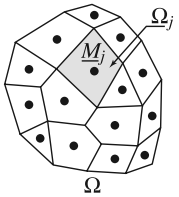

drastically reduced. Following [50], we are going to show the potential advantages of this framework.

Let us divide the time interval I being studied into m subintervals $\{I_i\}_{i=1,\dots,m}$ of lengths $\{\Delta t_i\}_{i=1,\dots,m}$ as shown in Fig. 5. Introducing the centers $\{t_i\}_{i=1,\dots,m}$ of these subintervals, called "reference times", one has $I_i = [t_i - \Delta t_i/2, t_i + \Delta t_i/2]$.

In the space domain, let us also introduce m' points $\{\underline{M}_j\}_{j=1,\dots,m'}$ and partition Ω into $\{\Omega_j\}_{j=1,\dots,m'}$ as shown in Fig. 6. These points are called "reference points" and the measures of the subdomains are denoted $\{\omega_j\}_{i=j,\dots,m'}$. In practice, there would usually be a few dozen reference points.

The choice of these reference times and reference points is unrelated to the classical discretizations of the time interval I and space domain Ω. Refined time and space discretizations should still be used for the calculation of the various quantities. Here, our purpose is to describe a field f over the time-space domain $I \times \Omega$ through:

$$\hat{a}_i^j(t) = \begin{cases} f(t, \underline{M}_j) & \text{if } t \in I_i \\ 0 & \text{otherwise} \end{cases} \quad \text{and}$$
$$\hat{b}_i^j(\underline{M}) = \begin{cases} f(t_i, \underline{M}) & \text{if } \underline{M} \in \Omega_j \\ 0 & \text{otherwise} \end{cases} \tag{36}$$

with $i = 1, \dots, m$ and $j = 1, \dots, m'$.

The sets $\{(\hat{a}_i^j, \hat{b}_i^j)\}_{i=1,\dots,m}^{j=1,\dots,m'}$ are the generalized components of f. One should note that these quantities verify the following compatibility conditions: for $i = 1, \dots, m$ and $j = 1, \dots, m'$,

$$\hat{a}_i^j(t_i) = \hat{b}_i^j(\underline{M}_j) \tag{37}$$

Then, the main question is: how can one build or rebuild a field from its components? We choose to define function f from its components using only one product per time-space subdomain $I_i \times \Omega_j$:

$$f(t, \underline{M}) : a_i^j(t) b_i^j(\underline{M}) \quad \forall (t, \underline{M}) \in I_i \times \Omega_j \tag{38}$$

where the sets $\{(a_i^j, b_i^j)\}_{i=1,\dots,m}^{j=1,\dots,m'}$ should be defined from the sets $\{(\hat{a}_i^j, \hat{b}_i^j)\}_{i=1,\dots,m}^{j=1,\dots,m'}$. However, in this case, we let the time domain play a special role because there are many more spatial degrees of freedom than there are time degrees of freedom. Thus, function f is defined by:

$$f(t, \underline{M}) : a_i(t) b_i(\underline{M}) \quad \forall (t, \underline{M}) \in I_i \times \Omega \tag{39}$$

Let us introduce the following scalar products:

$$\langle f, g \rangle_{I_i} = \int_{I_i} f g \, dt \quad \text{and} \quad \langle f, g \rangle_{\Omega_j} = \int_{\Omega_j} f g \, d\Omega \tag{40}$$

In order to obtain the sets $\{(a_i, b_i)\}_{i=1,\dots,m}$, we minimize:

$$J(a_i, b_i) = \sum_{j=1}^{m'} \Big[\omega_j \| \hat{a}_i^j(t) - a_i(t) b_i(\underline{M}_j) \|_{I_i}^2 + \Delta t_i \, \| \hat{b}_i^j(\underline{M}) - a_i(t_i) b_i(\underline{M}) \|_{\Omega_j}^2 \Big] \tag{41}$$

which leads to:

$$a_i(t) = \frac{\sum_{j=1}^{m'} \omega_j \hat{a}_i^j(t) b_i(\underline{M}_j)}{\sum_{j=1}^{m'} \omega_j b_i^2(\underline{M}_j)} \quad \text{and}$$
$$b_i(\underline{M}) = \frac{\sum_{j=1}^{m'} \hat{b}_i^j(\underline{M})}{m' a_i(t_i)} \tag{42}$$

Consequently, $\forall (t, \underline{M}) \in I_i \times \Omega_j$, we obtain:

$$f(t, \underline{M}) : a_i(t) b_i(\underline{M}) = \frac{\sum_{k=1}^{m'} \omega_k \hat{a}_i^k(t) \hat{b}_i^k(\underline{M}_k)}{\sum_{k=1}^{m'} \omega_k \hat{b}_i^k(\underline{M}_k) \hat{b}_i^k(\underline{M}_k)} \hat{b}_i^j(\underline{M}) \tag{43}$$

Then, using the compatibility conditions (37), we get:

$$f(t, \underline{M}) : a_i(t) b_i(\underline{M}) = \frac{\sum_{k=1}^{m'} \omega_k \hat{a}_i^k(t) \hat{a}_i^k(t_i)}{\sum_{k=1}^{m'} \omega_k \hat{a}_i^k(t_i) \hat{a}_i^k(t_i)} \hat{b}_i^j(\underline{M}) \tag{44}$$

4.5 Engineering Applications

The LATIN method described in Sect. 3 associated, at least partially, with the PGD method developed in Sect. 4 has enabled us to solve a number of industrial problems which would otherwise have been inaccessible with standard computation means. In [9], it was used in the context of assembly problems involving a large number of contacts. In [37], it was used as the basis of a local/global strategy for the simulation of crack propagation. In [10], it was used for the parametric analysis of bolted joints designed for aerospace applications. In [17], the method was used to develop a local/global strategy in order to solve buckling problems. In [8], a virtual testing tool was introduced in order to predict

damping in the joints of the Ariane 5 launcher. Finally, in [82], the method enabled the simulation of composite materials whose behavior was described on a microscale.

5 A Computational Strategy for Time-Space Multiscale Problems

5.1 Justification

In this section, we review how Proper Generalized Decomposition within the LATIN framework was used in [52, 56, 72] to analyze problems involving two or more very different scales. This is typically the case when domain Ω in Fig. 2 is highly heterogeneous and the local solution involves short-wavelength phenomena in both space and time. Attempting to solve such problems with classical finite element codes leads to systems with very large numbers of degrees of freedom, and the associated computation costs are generally prohibitive. Therefore, one of today's main challenges is to derive computational strategies capable of solving such engineering problems through true interaction between the microscale and the macroscale in both space and time.

The key issue is the transfer of information from one scale to the other. A very efficient strategy for linear periodic media consists in applying the homogenization theory introduced by Sanchez-Palencia [77, 78], for which additional developments and related computational approaches can be found in [18, 29, 31, 57, 73, 84]. First, the resolution of the macro problem leads to effective values of the unknowns; then, the micro solution is calculated locally based on the macro solution. The fundamental assumption, besides periodicity, is that the ratio of the characteristic length of the microscale to that of the macroscale is small. Boundary zones, in which the material cannot be homogenized, require special treatment. Moreover, this theory cannot be applied directly to time-dependent nonlinear problems. Other computational strategies using homogenization techniques based on the Hill-Mandel conditions [40] have also been proposed [44, 83], but have similar limitations. Other paradigms for building multiscale computational strategies can be found in [41, 53]. All these approaches introduce different scales in space alone.

Comparatively fewer works have been devoted to multi-time-scale computational strategies. What one calls multi-time-step methods [14, 25, 34, 35] and time-decomposed parallel time integrators [5, 22] deal with different time discretizations and integration schemes. Local enrichment functions were introduced in [7]. In multiphysics problems, a coupling among time grids may be envisaged. This type of problem was solved in [20] by introducing "micro/macro projectors" among grids. Some works have been devoted to the treatment of periodic loading histories [1, 13, 15, 30, 36, 46, 49].

Regarding the LATIN method, a micro/macro computational strategy involving space homogenization alone was introduced in [53]. This technique was later expanded in [52] to include time as well as space. The advantages of using PGD in this context were described in [72], and a more efficient and robust version of that strategy in the case of material models with internal variables was introduced in [56]. The following presentation covers only the main points. A comparison with other multiscale strategies can be found in [54].

5.2 Substructuring of the Problem

In order to take advantage of parallel computing and derive a multiscale strategy in time, the time domain I is divided into a small number of coarse subintervals $I_i^C = [t_i^C, t_{i+1}^C]$ (see Fig. 7). In the space domain, we follow the classical framework of domain decomposition methods and decompose the structure Ω into an assembly of substructures Ω_E[1] and interfaces $\Phi_{EE'}$[2] as shown on Fig. 7.

The state of a substructure Ω_E is defined entirely by $\dot{\mathbf{e}}_{pE}$ and $\mathbf{f}_E$, the restriction of fields $\dot{\mathbf{e}}_p$ and $\mathbf{f}$ to Ω_E. The state of an interface $\Phi_{EE'}$ is defined by its own variables—the velocity distributions $(\underline{\dot{W}}_E, \underline{\dot{W}}_{E'})$ and force distributions $(\underline{F}_E, \underline{F}_{E'})$ on both sides of the interface—and its own behavior. This behavior consists of the equilibrium condition (the action-reaction principle) plus a constitutive relation, defined by operator $\mathbf{b}_{EE'}$, which characterizes the behavior of the interface. In other words, the pairs of fields $(\underline{\dot{W}}_E, \underline{\dot{W}}_{E'})$ and $(\underline{F}_E, \underline{F}_{E'})$ must verify:

$$\begin{aligned} &\underline{F}_E + \underline{F}_{E'} = \underline{0} \\ &\mathbf{b}_{EE'}(\underline{\dot{W}}_E, \underline{\dot{W}}_{E'}, \underline{F}_E, \underline{F}_{E'}) = 0 \end{aligned} \tag{45}$$

In the case of a perfect connection, (45) is very simple and can be expressed as follows:

$$\begin{aligned} &\underline{F}_E + \underline{F}_{E'} = \underline{0} \\ &\underline{\dot{W}}_E - \underline{\dot{W}}_{E'} = \underline{0} \end{aligned} \tag{46}$$

In the case of unilateral contact with or without friction, the reader can refer to [19] for a detailed expression of operator $\mathbf{b}_{EE'}$. The interface concept can also be extended to the boundary of Ω over which a surface displacement distribution or a surface force distribution is prescribed. In order to

[1] The notation $\square_E$ designates the restriction of a quantity $\square$ to substructure Ω.

[2] $\Phi_{EE'}$ designates the interface between two substructures Ω_E and $\Omega_{E'}$.

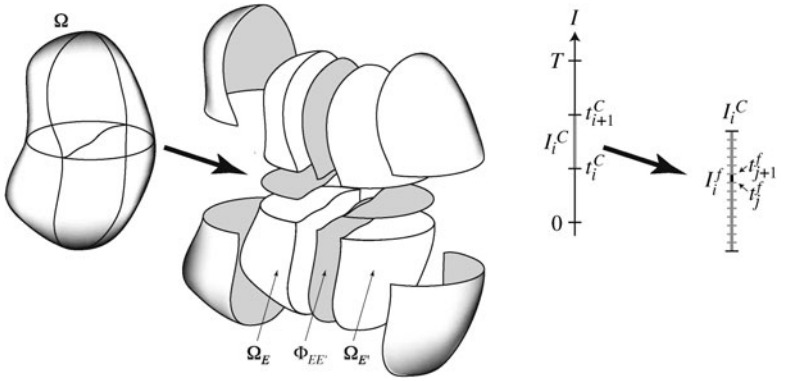

Fig. 7 Decomposition of Ω into substructures Ω_E and interfaces $\Phi_{EE'}$, and decomposition of I into subintervals I_i^C

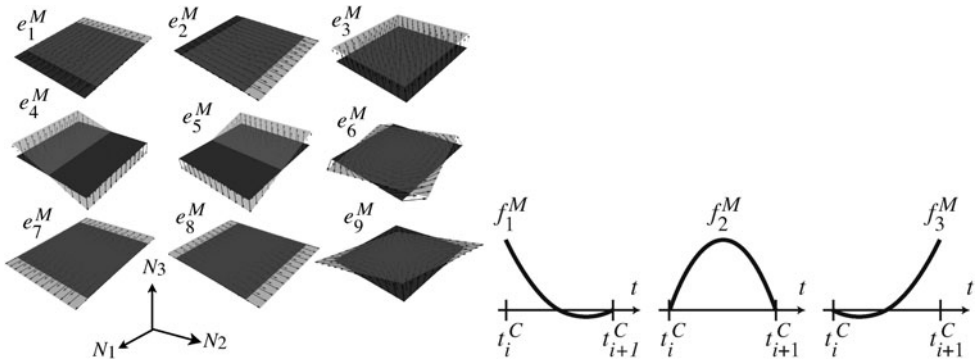

Fig. 8 The linear macro basis in space for a square interface $\Phi_{EE'}$ in the 3D case, and the quadratic macro basis in time over I_i^C

do that, one simply takes $\underline{W}_E = \underline{U}_d$ for a displacement prescribed over $\Phi_{E1} = \partial\Omega_E \cap \partial_1\Omega$, and $\underline{F}_E = \underline{F}_d$ for a force prescribed over $\Phi_{E2} = \partial\Omega_E \cap \partial_2\Omega$.

Let $\mathbf{s}_E = (\dot{\mathbf{e}}_{pE}, \underline{\dot{W}}_E, \mathbf{f}_E, \underline{F}_E)$ denote the set of the fields which describe the state of substructure Ω_E and its boundary $\partial\Omega_E$, and let $\mathbf{E}_E$, $\boldsymbol{\mathcal{W}}_E$, $\mathbf{F}_E$ and $\boldsymbol{\mathcal{F}}_E$ denote the corresponding spaces. The problem consists in finding $\mathbf{s} = (\mathbf{s}_E)_{\Omega_E \subset \Omega}$.

5.3 A Two-Scale Description of the Unknowns

Two scales, denoted the "macro" scale ($\square^M$) and the "micro" scale ($\square^m$) are introduced in order to describe the interface unknowns. This approach is physically consistent: the macro quantities are mean values over space and time, and due to Saint Venant's principle the effects of the micro complements are localized in space. $\forall \underline{F}^{M\star} \in \boldsymbol{\mathcal{F}}_E^M$, the macro part $\underline{\dot{W}}_E^M$ and the micro complement $\underline{\dot{W}}_E^m$ of $\underline{\dot{W}}_E \in \boldsymbol{\mathcal{W}}_E$ are defined by:

$$\int_{I_i^C \times \partial\Omega_E} (\underline{\dot{W}}_E^M - \underline{\dot{W}}_E) \cdot \underline{F}^{M\star}\, dSdt = 0 \quad \text{and}$$
$$\underline{\dot{W}}_E^m = \underline{\dot{W}}_E - \underline{\dot{W}}_E^M \tag{47}$$

where the spaces $\boldsymbol{\mathcal{F}}_E^M$ and $\boldsymbol{\mathcal{W}}_E^M$ can be chosen arbitrarily. In practice, these spaces are defined by the linear part in space and the quadratic part in time of the forces and displacements (see Fig. 8 for the shape of the corresponding basis functions).

An important point of the strategy which leads to its multiscale character is the choice of the admissibility conditions for the macro quantities. The set of the macro forces $(\underline{F}_E^M)_{\Omega_E \subset \Omega}$ is required to verify *a priori* the transmission conditions, including the boundary conditions, systematically:

$$\begin{aligned} &\underline{F}_E^M + \underline{F}_{E'}^M = \underline{0} \quad \text{over } \Phi_{EE'} \\ &\underline{F}_E^M - \underline{F}_d^M = \underline{0} \quad \text{over } \Phi_{E2} = \partial_E\Omega \cap \partial_2\Omega \end{aligned} \tag{48}$$

The corresponding subspace of $\boldsymbol{\mathcal{F}}^M = \bigotimes \boldsymbol{\mathcal{F}}_E^M$ is designated by $\boldsymbol{\mathcal{F}}_{ad}^M$. We use the same definition for $\boldsymbol{\mathcal{W}}^M$ and $\boldsymbol{\mathcal{W}}_{ad}^M$.

5.4 Reformulation of the Reference Problem in the Decomposed Framework

Now let us extend the definition of the spaces $\boldsymbol{\mathcal{U}}$, $\boldsymbol{\mathcal{F}}$, $\boldsymbol{\mathcal{E}}$ and $\mathbf{A_d}$ introduced in Sect. 3 in order to reformulate the problem in the decomposed framework. In order to do that, we introduce the following new functional subspaces (whose definitions are obvious):

- *the space $\boldsymbol{\mathcal{U}}_E$ of the kinematically admissible fields* $(\mathbf{u}_E, \underline{W}_E)$, whose displacements $\underline{W}_E$ over $\partial\Omega_E$ are equal to field $\underline{U}_E$ and which verify the initial conditions $\underline{U}_{E0}$: $\underline{U}_{E|\partial\Omega_E} = \underline{W}_E$ and $\underline{U}_{E|t=0} = \underline{U}_{E0}$

- *the space* $\mathcal{F}_E$ *of the statically admissible fields* $(\mathbf{f}_E, \underline{F}_E)$, whose stress fields $\boldsymbol{\sigma}_E$ are in equilibrium with the interface forces $\underline{F}_E$ over $\partial\Omega_E$ and which verify the momentum conservation equation:

$$\forall (\mathbf{u}^\star_E, \underline{W}^\star_E) \in \mathcal{U}^\star_E,$$
$$-\int_{I_i^C\times\Omega_E} \mathbf{f}_E \circ \mathbf{e}(\dot{U}^\star_E)\, d\Omega dt + \int_{I_i^C\times\Omega_E} \underline{f}_d \cdot \dot{\underline{U}}^\star_E\, d\Omega dt$$
$$+\int_{I_i^C\times\partial\Omega_E} \underline{F}_E \cdot \dot{\underline{W}}^\star_E\, dSdt = 0 \tag{49}$$

- *the space* $\boldsymbol{\mathcal{E}}_E$ *of the kinematically admissible fields* $(\dot{\mathbf{e}}_E, \dot{\underline{W}}_E)$, whose strain fields $\boldsymbol{\varepsilon}_E$ derive from displacement fields $(\underline{U}_E, \underline{W}_E)$ belonging to $\boldsymbol{\mathcal{U}}_E$:

$$\forall (\mathbf{f}^\star_E, \underline{F}^\star_E) \in \boldsymbol{\mathcal{F}}^\star,$$
$$-\int_{I_i^C\times\Omega_E} \mathbf{f}^\star_E \circ \dot{\mathbf{e}}_E\, d\Omega dt$$
$$+\int_{I_i^C\times\partial_1\Omega_E} \underline{F}^\star_E \cdot \dot{\underline{W}}_E\, dSdt = 0 \tag{50}$$

- *the space* $\mathbf{A}_{\mathbf{d}E}$ *of the* E*-admissible fields* $\mathbf{s}_E$ in which $(\mathbf{f}_E, \underline{F}_E)$ is statically admissible, $\mathbf{f}_E$ and $\dot{\mathbf{e}}_{pE}$ verify the state law (13), and the corresponding $(\dot{\mathbf{e}}_E, \dot{\underline{W}}_E)$ is kinematically admissible:

$$(\mathbf{f}_E, \underline{F}_E) \in \boldsymbol{\mathcal{F}}_E, \quad (\mathbf{A}^{-1}\dot{\mathbf{f}}_E + \dot{\mathbf{e}}_{pE}, \dot{\underline{W}}_E) \in \boldsymbol{\mathcal{E}}_E \tag{51}$$

Then, we also redefine:

- *the space* $\mathbf{A}_{\mathbf{d}}$ *of the admissible fields* $\mathbf{s} = (\mathbf{s}_E)_{\Omega_E\subset\Omega}$ in which each $\mathbf{s}_E$ is E-admissible and the macro forces verify the transmission conditions (48):

$$\forall \Omega_E \subset \Omega, \quad \mathbf{s}_E \in \mathbf{A}_{\mathbf{d}E} \quad \text{and} \quad (\underline{F}^M_E)_{\Omega_E\subset\Omega} \in \boldsymbol{\mathcal{F}}^M_{ad} \tag{52}$$

- *the space* $\boldsymbol{\Gamma}$ *of the fields* $\mathbf{s} = (\mathbf{s}_E)_{\Omega_E\subset\Omega}$ in which $\mathbf{f}_E$ and $\dot{\mathbf{e}}_{pE}$ verify the evolution law (14) and $(\underline{F}_E, \underline{F}_{E'}, \dot{\underline{W}}_E, \dot{\underline{W}}_{E'})$ verify the interface behavior (45):

$$\forall \Omega_E \subset \Omega, \quad \dot{\mathbf{e}}_{pE} = \mathbf{B}(\mathbf{f}_E) \quad \text{and}$$
$$\forall \Phi_{EE'}, \begin{cases} \underline{F}_E + \underline{F}_{E'} = \underline{0} \\ \mathbf{b}_{EE'}(\dot{\underline{W}}_E, \dot{\underline{W}}_{E'}, \underline{F}_E, \underline{F}_{E'}) = 0 \end{cases} \tag{53}$$

Obviously, the solution $\mathbf{s}_{\mathbf{ref}}$ of the problem over the time-space domain $I \times \Omega$ is the intersection of $\mathbf{A}_{\mathbf{d}}$ and $\boldsymbol{\Gamma}$. Thus, the reference problem becomes:

$$\text{Find } \mathbf{s}_{\mathbf{ref}} \in \mathbf{A}_{\mathbf{d}} \cap \boldsymbol{\Gamma} \tag{54}$$

5.5 The LATIN Method as a Solver

The previous problem is solved using the LATIN method as described in Sect. 3. In order to do that, one must introduce in the search directions $\mathbf{E}^+$ and $\mathbf{E}^-$ some additional terms corresponding to the boundary fields:

$$\mathbf{E}^+ = \left\{ \delta\mathbf{s} = (\delta\mathbf{s}_E)_{\Omega_E\subset\Omega} \,\middle|\, \begin{matrix} \delta\dot{\mathbf{e}}_{pE} + \mathbf{H}^+\delta\mathbf{f}_E = 0 \\ \delta\dot{\underline{W}}_E - \mathbf{h}^+\delta\underline{F}_E = \underline{0} \end{matrix} \right\} \tag{55}$$

and

$$\mathbf{E}^- = \left\{ \delta\mathbf{s} = (\delta\mathbf{s}_E)_{\Omega_E\subset\Omega} \,\middle|\, \begin{matrix} \delta\dot{\mathbf{e}}_{pE} - \mathbf{H}^-\delta\mathbf{f}_E = 0 \\ \delta\dot{\underline{W}}_E + \mathbf{h}^-\delta\underline{F}_E = \underline{0} \end{matrix} \right\} \tag{56}$$

where $\mathbf{h}^+$ and $\mathbf{h}^-$ are symmetric, positive definite operators which are parameters of the method and which are usually set to be equal to $\mathbf{h}^+ = \mathbf{h}^- = \mathbf{h}$. In the case of linear behavior, one can choose $\mathbf{h} = \frac{L}{ET}\mathbf{I}$, where E is the Young's modulus of the material, L_E a characteristic length of the interfaces, T the duration of the phenomenon being studied and $\mathbf{I}$ the identity operator. Other possible choices, especially in the nonlinear case, are discussed in [51].

Then, the local stage becomes very similar to that described in Sect. 3, but the linear stage requires special treatment. The admissibility of the macro forces $(\underline{F}^M_E)_{\Omega_E\subset\Omega} \in \boldsymbol{\mathcal{F}}^M_{ad}$ (and, consequently, the verification of the transmission conditions (48)) is obtained by introducing a Lagrange multiplier $\underline{\tilde{W}}^M = (\underline{\tilde{W}}^M_E)_{\Omega_E\subset\Omega} \in \boldsymbol{\mathcal{W}}^{M\star}_{ad}$. This Lagrange multiplier is obtained by solving a homogenized linear time-space "macro" problem defined over the whole set of interfaces and the entire coarse subinterval I_i^C. Once this macro field is known, the complete solution $\mathbf{s} = (\mathbf{s}_E)_{\Omega_E\subset\Omega}$ is obtained by solving a set of "micro" problems defined over each time-space domain $I_i^C \times \Omega_E$. The detailed treatment of the linear stage using the PGD framework can be found in [56].

5.6 An Illustrative Example

The following example, taken from [55], illustrates the different steps of the LATIN multiscale strategy and the effectiveness and efficiency of the PGD technique in the resolution of the micro problems introduced previously.

5.6.1 Illustration of the LATIN Multiscale Strategy

Let us consider the 3D problem of a composite structure with cracks (see Fig. 9(a)). This structure is fixed at the base and subjected to forces $\underline{F}_1$, $\underline{F}_3$ and $\underline{F}_3$ (see Fig. 9(b)). The overall dimensions are $120 \times 120 \times 20$ mm, and the time interval being studied is $T = 10$ s. The cracks are described using unilateral contact with Coulomb friction characterized by parameter $f = 0.3$.

The structure consists of two types of cells: Type-I cells, which are homogeneous and made of a material denoted Type-1, and Type-II cells composed of a matrix of Type-1 material with inclusions of a material denoted Type-2. Both

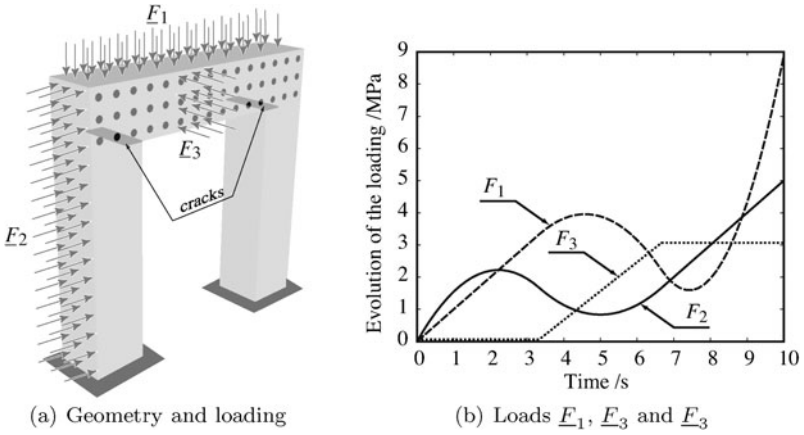

Fig. 9 Description of the problem

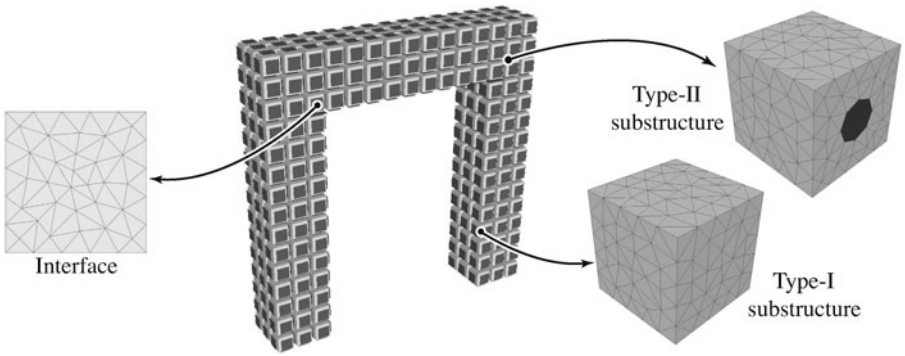

Fig. 10 Decomposition into substructures and interfaces and spatial discretization on the microscale

Table 1 Material properties

Material	Type-1	Type-2
Young's modulus	$E_1 = 50$ GPa	$E_2 = 250$ GPa
Poisson's ratio	$\nu_1 = 0.3$	$\nu_2 = 0.2$
Viscosity parameter	$\eta_1 = 10$ s	$\eta_2 = 1{,}000$ s

materials are viscoelastic and their properties are given in Table 1. The corresponding constitutive relations are $\dot{\boldsymbol{\varepsilon}}_p = \mathbf{B}_i\boldsymbol{\sigma} = \frac{1}{\eta_i}\mathbf{K}_i^{-1}\boldsymbol{\sigma}$.

As shown in Fig. 10, the problem was divided into 351 substructures (each substructure corresponding to one cell) and 1,296 interfaces. On the micro level, Type-I and Type-II substructures and their interfaces were meshed with 847, 717 and 144 degrees of freedom (DOFs) respectively. In the space domain, the macro part consisted of a single linear element per interface with only 9 DOFs. With respect to time, the micro level was associated with a refined discretization into 60 intervals using a zero-order discontinuous Galerkin scheme, and the macrolevel was associated with a coarse discretization into 3 macro intervals using a second-order discontinuous Galerkin scheme. Because of the linearity of the constitutive relation, the search direction chosen for the substructures was $\mathbf{H} = \mathbf{B}$. With the characteristic length of the interfaces being $L_E = 4$ mm, we chose the search direction $\mathbf{h} = h\mathbf{I}$ for all the interfaces, $h = \frac{L_E}{E_1\nu_1}$ being a constant scalar.

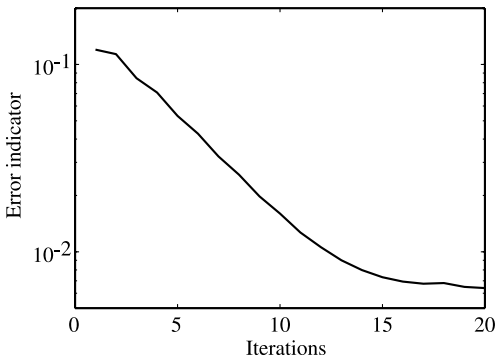

Fig. 11 Convergence of the method

Figure 11 shows the evolution of the error indicator η with the number of iterations. One can observe that the algorithm converges rapidly toward an accurate solution (1% error after 12 iterations). Figure 12 shows the approximate Von Mises stress fields over the structure at the final time $T = 10$ s (with a zoom near one of the cracks) at Iterations 1, 5 and 20 and after convergence (the reference solution) and also shows the evolution over time of the displacement field $\underline{W}$ at point P_2. One can observe that even after the first iteration, thanks to the resolution of the macro problem, the method yields a relatively good approximate solution of the

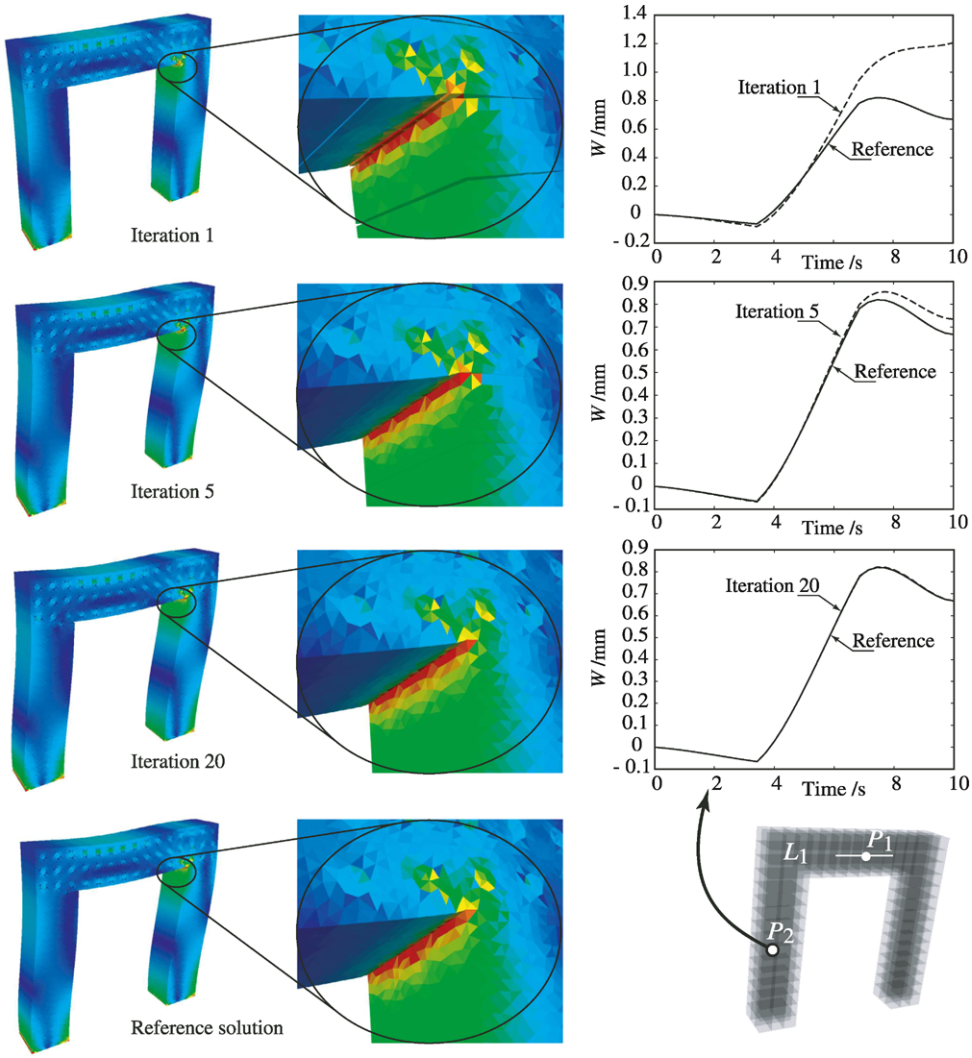

Fig. 12 Approximate solutions after various numbers of iterations

problem in both the space domain and the time domain. After a few iterations, the solution becomes even more accurate and the stress and displacement discrepancies tend toward zero. After 20 iterations, the difference between the approximate solution and the reference solution is no longer visible.

5.6.2 *Illustration of the Use of the PGD Technique*

In order to illustrate how the PGD technique was used in the multiscale strategy, let us examine the treatment of one of the micro problems in detail. The micro problem being considered is defined over $I_i^C \times \Omega_E$, where Ω_E corresponds to one of the Type-II substructures of Fig. 10. The loading is represented by the distribution of the Lagrange multiplier $\underline{\widetilde{W}}_E^M$ alone. For the sake of simplicity, we assume that this loading consists of only a normal force distribution $f(t)$ over the upper surface of the substructure (see Fig. 13).

Figure 14 shows the evolution of the constitutive relation error e_{CR}^2 associated with the search direction versus the

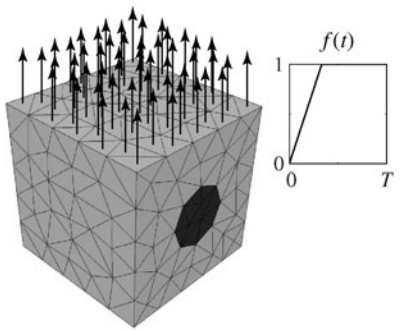

Fig. 13 Description of a micro problem corresponding to a Type-II substructure and its loading

number of functions, obtained using two techniques: in the first technique, new pairs of time/space functions were built systematically; the second technique consisted, as described in Algorithm 1, in first reusing the reduced basis of space functions calculated previously to update the time functions alone, and only after that seeking a new pair of time/space

functions. One can see that the accuracy of the approximation is very good because with only 4 radial functions the error was less than 1%. However, one can observe that the convergence rate was higher with the second technique than with the first. For example, in order to get less than 0.1% error, 15 functions needed to be calculated without updating the time functions, as opposed to only 8 functions using the updating procedure. Since the computation cost associated with reusing the reduced basis is much less than the cost associated with an additional space function, it is very important to update the time functions systematically.

Figure 15, shows the first four pairs consisting of a space function and a time function. Since the space functions are normalized, one can observe a decrease in the level of the corresponding time functions. Figure 16 shows a comparison of the Von Mises stress distributions over the space and time domains obtained with the radial time-space approximation and the classical incremental technique.

A very important point is that although the basis of the space functions is *a priori* specific to the problem and the loading for which it was defined, it can be reused to solve another problem with comparable accuracy. For example, we solved the previous micro problem with 6 functions and reused these functions for all the loading cases of Fig. 17. In order to do that, we carried out a single updating stage and evaluated the corresponding error.

Table 18 shows that by updating the time functions alone using the same space functions as for a previous problem $f(t)$ one obtains an approximate solution of the new problem $f_i(t)$ with an accuracy comparable to that of the first problem. The robustness of the PGD approximation makes it well-adapted to multiresolution and, thus, this approximation technique is quite suitable for the multiscale strategy, which involves the resolution of a set of micro problems at each iteration of the LATIN method. We can reuse the same basis at every iteration of these micro problems, and even consider using a common basis for the whole set of substructures.

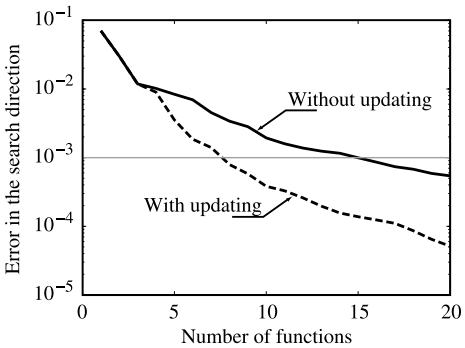

Fig. 14 Convergence of the PGD approximation

6 A Computational Strategy for Multiphysics Problems

6.1 Justification

In this section, we review how Proper Generalized Decomposition within the LATIN framework was used in [20, 21, 68] to deal with multiphysics problems. This is typically the case when domain Ω of Fig. 2 is made of a porous material whose physics involve the fluid phase in connected porosities and the solid phase as the skeleton of the porous medium.

Partitioning approaches, which consist basically in separating the physics in order to avoid the simultaneous treatment of the different fields, are usually preferred to the direct monolithic analysis [6, 33, 65] because they offer several interesting features including: (i) the ability to use different discretizations for each physics; (ii) a simplification in software development efforts; (iii) the preservation of software modularity. These advantages have been reported in relation to a broad range of coupled multiphysics problems, such as fluid/structure interactions in [23, 26, 27, 58, 59, 66, 74] and others. In particular, the issue of the exchange of

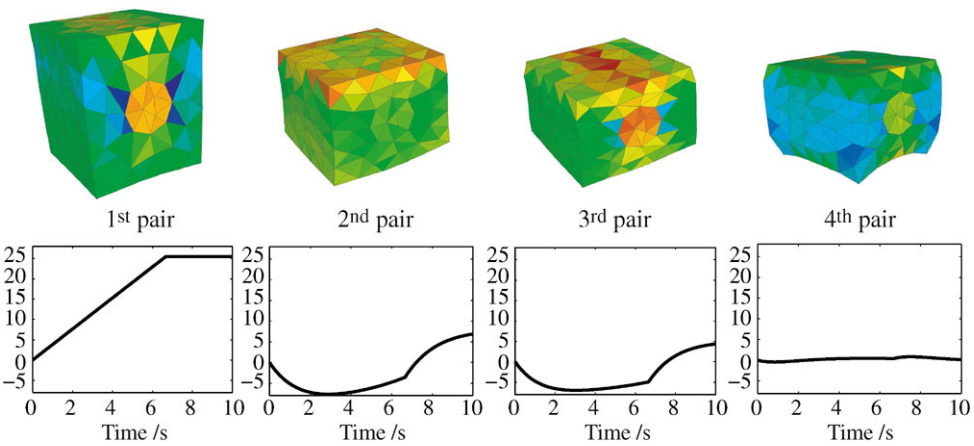

Fig. 15 The first four radial time-space functions for the problem

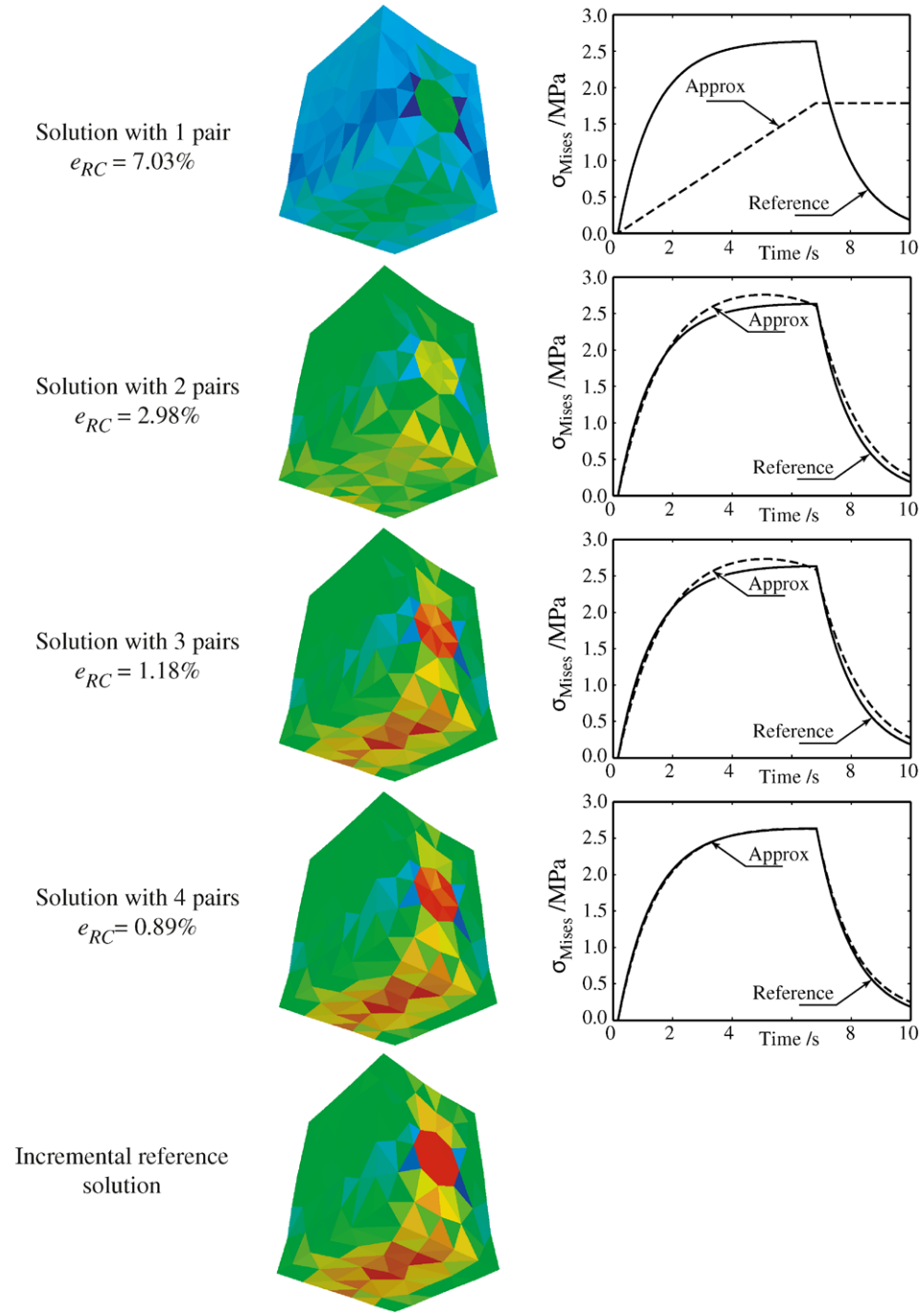

Fig. 16 Quality of the approximations with 1, 2, 3 and 4 pairs

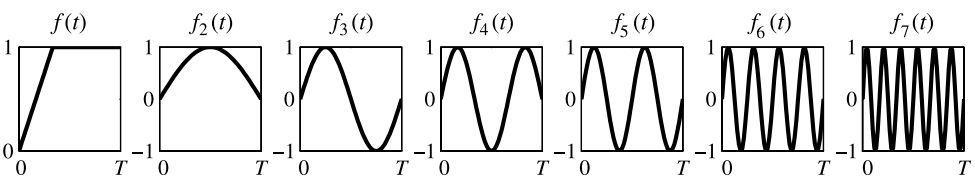

Fig. 17 The different loading cases for the micro problem

Loading case	$f(t)$	$f_2(t)$	$f_3(t)$	$f_4(t)$	$f_5(t)$	$f_6(t)$	$f_7(t)$
Error e_{CR}	0.179%	0.183%	0.239%	0.291%	0.332%	0.411%	0.434%

Fig. 18 Reutilization of a space function with the PGD approximation

data between two different physics was studied using several different approaches in [23, 74], and the possibility of using different treatments (computer programs, integration schemes...) for the different physics involved was highlighted in [4, 24, 28, 62, 64, 74, 85].

The feasibility of using the LATIN method to derive a partitioning approach to deal with multiphysics problems was presented in [21] for the case of a two-physics problem (the transient saturated poroelastic evolution of a medium). The treatment of nonlinear behavior was presented in [69]. For the same problem, the possibility of coupling different time discretizations using a fixed-point method between the two physics was described in [20]. However, such a procedure requires numerous field transfer operations between the physics, which can lead to expensive computations. This was the motivation behind the attempt to extend the approach by introducing the concept of interface among physics, which was applied to different time discretizations in [67]. The extension to a three-physics problem (nonlinear thermo-poroelasticity) along with the introduction of different discretizations in both time and space was presented in [68]. In all these works, the use of PGD enabled a reduction not only in computation cost, but also in the amount of data which must be transferred from one physics to another. The following presentation is limited to a review of the main points in the case of a two-physics problem.

6.2 The Reference Problem

Let us consider the example case of the coupled two-physics problem of the quasi-static poroelastic evolution of a saturated porous medium in the time-space domain $I \times \Omega$. Under the assumption of small perturbations, the state of the structure is defined, for the solid part, by the strain field $\boldsymbol{\varepsilon}$ corresponding to the displacement field $\underline{U}$ and associated with the stress field $\boldsymbol{\sigma}$, and, for the fluid part, by the pore pressure field p associated with the fluid accumulation field v in the representative volume element and Darcy's velocity $\underline{w}$.

The homogenized poroelastic behavior of the material is described in [16, 58]. The *state laws* are:

$$\begin{aligned} \boldsymbol{\sigma} &= \mathbf{K}\boldsymbol{\varepsilon} - bp\mathbf{I} \\ v &= \frac{1}{Q}p + b\,\mathrm{Tr}\,\boldsymbol{\varepsilon} \end{aligned} \tag{57}$$

However, we prefer to use the rate of fluid accumulation $q = \dot{v}$ instead of the fluid accumulation itself, *i.e.*:

$$q = \frac{1}{Q}\dot{p} + b\,\mathrm{Tr}\,\dot{\boldsymbol{\varepsilon}} \tag{58}$$

We also introduce $\underline{Z} = \underline{\mathrm{grad}}\, p$, the gradient of the pore pressure p, and $\underline{W} = -\underline{w}$, the opposite of Darcy's velocity $\underline{w}$, so the *evolution law* becomes:

$$\underline{W} = \mathbf{H}\underline{Z} \tag{59}$$

The coefficients of the material behavior model are: the Hooke's operator $\mathbf{K}$ of the drained skeleton, which, in the case of isotropic behavior, depends on only two coefficients (e.g. the Young's modulus E and Poisson's ratio ν); the bulk modulus $K_b = \frac{1}{3}E/(1-2\nu)$ of the drained skeleton; Biot's coefficient $b = 1 - K_b/K_s$, where K_s is the bulk modulus of the solid phase (solid grains); Biot's modulus $Q = ((b-n)/K_b + n/K_F)^{-1}$ taking into account compressibility (n being the porosity and K_F the compressibility of the fluid phase); the permeability $\mathbf{H} = K/\mu_F$ of the porous media; the intrinsic permeability K of the skeleton; and the dynamic viscosity μ_F of the fluid phase.

In this reference problem, the loading consists of prescribed body forces within domain Ω, which we will assume to be zero for the sake of simplicity in our presentation; prescribed displacements $\underline{U}_d$ on a part $\partial_1\Omega$ of the boundary $\partial\Omega$ and traction forces $\underline{F}_d$ on the complementary part $\partial_2\Omega$ of $\partial\Omega$; and, finally, a prescribed pore pressure p_d on another part $\partial_3\Omega$ of the boundary and a fluid flux w_d on the complementary part $\partial_4\Omega$ of $\partial\Omega$. In order to determine the state of the structure $\mathbf{s} = (\mathbf{s}_S, \mathbf{s}_F)$ (where $\mathbf{s}_S = (\dot{\boldsymbol{\varepsilon}}, \boldsymbol{\sigma})$ are the fields corresponding to the solid and $\mathbf{s}_F = (p, \underline{Z}, q, \underline{W})$ the fields corresponding to the fluid), which is sought in $\mathbf{S}_S \times \mathbf{S}_F$, one must establish the conservation principles: momentum conservation for the solid part and mass conservation for the fluid part.

6.3 Partitioning of the Problem

In order to formulate the reference problem, let us introduce the following functional subspaces, using $\square^\star$ to denote vector spaces associated with affine spaces:

- *the space* $\boldsymbol{\mathcal{U}}$ *of the kinematically admissible fields* $\underline{U}$ which are equal to the prescribed displacements $\underline{U}_d$ over $\partial_1\Omega$: $\underline{U}_{|\partial_1\Omega} = \underline{U}_d$
- *the space* $\boldsymbol{\mathcal{F}}$ *of the statically admissible fields* $\boldsymbol{\sigma}$ which verify the momentum conservation equation and are in equilibrium with the external prescribed forces $\underline{F}_d$ over the complementary part $\partial_2\Omega$ of the boundary (for the sake of simplicity, we assume that there are no body forces):

$$\forall \underline{U}^\star \in \boldsymbol{\mathcal{U}}^\star,$$
$$-\int_{I\times\Omega} \boldsymbol{\sigma} : \boldsymbol{\varepsilon}(\dot{\underline{U}}^\star)\, d\Omega dt + \int_{I\times\partial_2\Omega} \underline{F}_d \cdot \dot{\underline{U}}^\star\, dS dt = 0 \tag{60}$$

- *the space* $\boldsymbol{\mathcal{E}}$ *of the kinematically admissible fields* $\dot{\boldsymbol{\varepsilon}}$ which derive from a displacement field $\underline{U}$ belonging to $\boldsymbol{\mathcal{U}}$:

$$\forall \boldsymbol{\sigma}^\star \in \boldsymbol{\mathcal{F}}^\star,$$

$$-\int_{I\times\Omega}\boldsymbol{\sigma}^\star:\dot{\boldsymbol{\varepsilon}}\,d\Omega dt+\int_{I\times\partial_1\Omega}\boldsymbol{\sigma}^\star\underline{n}\cdot\underline{\dot{U}}_d\,dSdt=0 \quad (61)$$

- *the space* $\mathbf{A}_{\mathbf{d}S}$ *of the S-admissible fields* $\mathbf{s}_S$ in which $\boldsymbol{\sigma}$ is statically admissible and $\dot{\boldsymbol{\varepsilon}}$ is kinematically admissible:

$$\boldsymbol{\sigma}\in\boldsymbol{\mathcal{F}} \quad \text{and} \quad \dot{\boldsymbol{\varepsilon}}\in\boldsymbol{\mathcal{E}} \quad (62)$$

- *the space* $\boldsymbol{\mathcal{P}}$ *of the kinematically admissible fields* p which are equal to the prescribed pressure p_d over $\partial_3\Omega$: $p_{|\partial_3\Omega}=p_d$.
- *the space* $\boldsymbol{\mathcal{W}}$ *of the statically admissible fields* $(q,\underline{W})$ which verify the mass conservation equation and balance the external prescribed flux w_d over $\partial_4\Omega$:

$$\forall p^\star\in\boldsymbol{\mathcal{P}}^\star,$$
$$-\int_{I\times\Omega}(qp^\star+\underline{W}\cdot\underline{\operatorname{grad}}\,p^\star)\,d\Omega dt+\int_{I\times\partial_4\Omega}w_d\,p^\star\,dSdt=0 \quad (63)$$

- *the space* $\boldsymbol{\mathcal{Z}}$ *of the kinematically admissible fields* $(p,\underline{Z})$ where $\underline{Z}$ derives from the pressure field p belonging to $\boldsymbol{\mathcal{P}}$:

$$\forall(q^\star,\underline{W}^\star)\in\boldsymbol{\mathcal{W}}^\star,$$
$$-\int_{I\times\Omega}(q^\star p+\underline{W}^\star\cdot\underline{Z})\,d\Omega dt+\int_{I\times\partial_3\Omega}\underline{W}^\star\cdot\underline{n}\,p_d\,dSdt=0 \quad (64)$$

- *the space* $\mathbf{A}_{\mathbf{d}F}$ *of the F-admissible fields* $\mathbf{s}_F$ in which $(q,\underline{W})$ is statically admissible and $(p,\underline{Z})$ is kinematically admissible:

$$(q,\underline{W})\in\boldsymbol{\mathcal{W}} \quad \text{and} \quad (p,\underline{Z})\in\boldsymbol{\mathcal{Z}} \quad (65)$$

Let us also define:

- *the space* $\mathbf{A}_{\mathbf{d}}$ *of the admissible fields* $\mathbf{s}=(\mathbf{s}_S,\mathbf{s}_F)$ where each $\mathbf{s}_S$ is S-admissible and $\mathbf{s}_F$ is F-admissible:

$$\mathbf{s}_S\in\mathbf{A}_{\mathbf{d}S} \quad \text{and} \quad \mathbf{s}_F\in\mathbf{A}_{\mathbf{d}F} \quad (66)$$

- *the space* $\boldsymbol{\Gamma}$ *of the fields* $\mathbf{s}=(\mathbf{s}_S,\mathbf{s}_F)$ which verify the state and evolution laws:

$$\boldsymbol{\sigma}=\mathbf{K}\boldsymbol{\varepsilon}-bp\mathbf{I}, \qquad q=\frac{1}{Q}\dot{p}+b\,\mathrm{Tr}\,\dot{\boldsymbol{\varepsilon}} \quad \text{and} \quad \underline{W}=\mathbf{H}\underline{Z} \quad (67)$$

Clearly, the solution $\mathbf{s}_{\mathbf{ref}}$ of the problem over the time-space domain $I\times\Omega$ is the intersection of $\mathbf{A}_{\mathbf{d}}$ and $\boldsymbol{\Gamma}$. Thus, the reference problem becomes:

$$\text{Find } \mathbf{s}_{\mathbf{ref}}\in\mathbf{A}_{\mathbf{d}}\cap\boldsymbol{\Gamma} \quad (68)$$

It is important to note that $\mathbf{A}_{\mathbf{d}}$ is a set of solutions of global linear equations in which the physics are uncoupled, whereas $\boldsymbol{\Gamma}$ is a set of solutions of coupled equations which are local in the space variable.

6.4 The LATIN Method as a Solver

The previous problem is solved using the LATIN method as described in Sect. 3. In order to do that, one must introduce specific search directions:

$$\mathbf{E}^+=\left\{\delta\mathbf{s}=(\delta\mathbf{s}_S,\delta\mathbf{s}_F)\;\middle|\;\begin{array}{l}\delta\dot{\boldsymbol{\varepsilon}}+\mathbf{L}\delta\boldsymbol{\sigma}=0\\ \delta p+r\delta q=0\\ \delta\underline{Z}-\mathbf{M}\delta\underline{W}=\underline{0}\end{array}\right\} \quad (69)$$

and

$$\mathbf{E}^-=\left\{\delta\mathbf{s}=(\delta\mathbf{s}_S,\delta\mathbf{s}_F)\;\middle|\;\begin{array}{l}\delta\dot{\boldsymbol{\varepsilon}}-\mathbf{L}\delta\boldsymbol{\sigma}=0\\ \delta p-r\delta q=0\\ \delta\underline{Z}-\mathbf{M}\delta\underline{W}=\underline{0}\end{array}\right\} \quad (70)$$

where $\mathbf{L}$, r and $\mathbf{M}$ are symmetric, positive definite operators which are parameters of the method. Since the behavior is linear, following [21], one can choose $\mathbf{L}=1/t_S\mathbf{K}$, $r=t_F Q$ and $\mathbf{M}=\mathbf{H}^{-1}$, where t_S and t_F are parameters whose choice is discussed in [67]. For the nonlinear case, one can refer to [68, 69].

This partitioning of the equations can be viewed as an extension of the concept of geometric interface used in domain decomposition methods to that of an "interface among physics" (see Fig. 19). This interface is defined in the time-space domain $I_I\times\Omega_I$ (T_I is a possible time discretization of this interface and Ω_I is the corresponding space discretization). The behavior of the interface consists in the verification of the constitutive relations which couple the physics, *i.e.* the group of equations $\boldsymbol{\Gamma}$. The solid and fluid time-space discretizations $I_S\times\Omega_S$ and $I_F\times\Omega_F$, which involve only parts $\mathbf{s}_S$ and $\mathbf{s}_F$ of the unknowns, are also defined. Their behavior consists in letting these unknowns verify the compatibility conditions and the conservation laws, *i.e.* the groups of equations $\mathbf{A}_{\mathbf{d}S}$ and $\mathbf{A}_{\mathbf{d}F}$. This enables one to choose different time and space discretizations of the unknowns for each physics and for the interface. This modularity is especially interesting when different simulation codes and solvers are used for the different physics.

The use of such an interface gives modularity properties to both the modeling of the coupled phenomena and the resolution process. For example, if a physical model changes or if a third physics is added, a corresponding time-space domain can be added and the new coupling properties enrich the interface behavior (see Fig. 20).

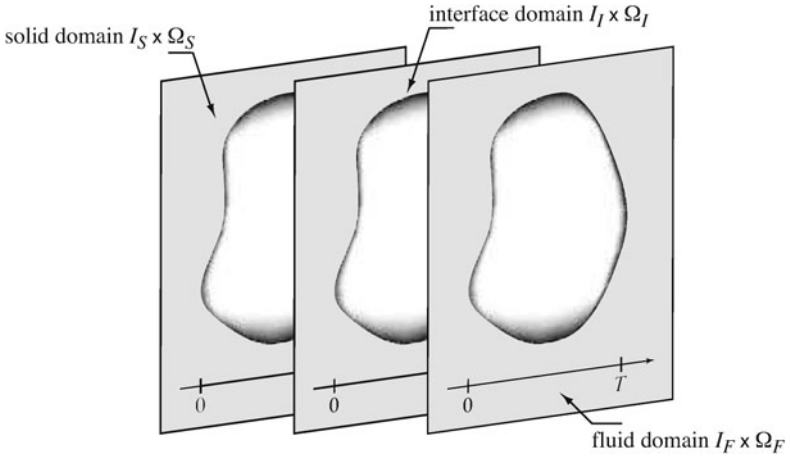

Fig. 19 An interface among physics defined over the whole domain

The advantage of using different time-space discretizations for the different physics is obvious. In [20] for example, it was shown that due to the different characteristic times of the phenomena it was unnecessary to perform all the calculations using the same time mesh in order to achieve the same accuracy in the solutions for the solid and for the fluid. A coarser discretization for the solid part was sufficient to achieve similar-quality results. A technical procedure for transferring fields from one discretization to another, especially when the meshes do not match, is described in [67, 68].

6.5 An Illustrative Example

The following example, taken from [20], illustrates the different steps of the LATIN strategy for multiphysics problems and the performance of the PGD approximation in the resolution of the uncoupled problems.

6.5.1 Illustration of the LATIN Multiscale Strategy

The proposed test case concerns the consolidation of a Berea sandstone soil (see Fig. 21). The material characteristics are presented in Table 2. The time interval is $T = 36$ s, with $t_1 = T/10$; the pressures are $p_1 = 1.54$ GPa and $p_0 = 380$ MPa; the initial condition is $p(t = 0) = p_0$.

The space discretization was performed using P2 elements (6-node triangles) for the displacements and P1 linear interpolation (also continuous across element boundaries) for the pore pressure. The θ-method with linear evolution of the variables with time was used for the time integration. [39, 81] propose the accuracy condition $\frac{\Delta t}{\Delta \ell^2} \geq \frac{1}{6\theta c}$, where Δt is the length of a time step, $\Delta \ell$ the size of a spatial element, and $c = E\frac{K}{\mu_w}\frac{3-2\nu}{3(1+\nu)(1-2\nu)}$. Here, since $\theta = 1$ everywhere, this condition leads to $\frac{\Delta t}{\Delta \ell^2} \geq 0.048\ \mathrm{sm}^{-2}$. The mesh used is shown in Fig. 21. The accuracy criterion was $(\frac{\Delta t}{\Delta \ell^2})_{\min} = 0.075\ \mathrm{sm}^{-2} > 0.048\ \mathrm{sm}^{-2}$, which verifies the previous condition.

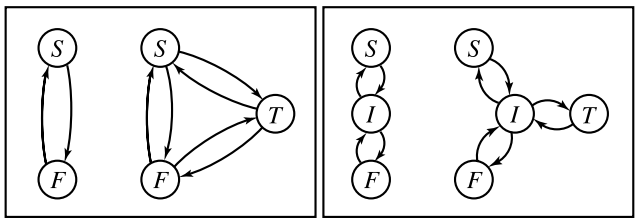

Fig. 20 Modification of the transfer operations with the addition of a new physics "T" (*left*: with no interface, *right*: with a dedicated interface)

Our objective is to compare the LATIN approach with the Iterative Standard Parallel Procedure (ISPP [63]), which is one of the standard partitioning schemes. In order to compare the results in terms of computation cost, let us introduce the following notations: as before, n_I is the number of time steps in the interval I being studied; n_S and n_F are the numbers of global uncoupled resolutions (*i.e.* the expensive parts of the algorithms) for the solid and for the fluid respectively. Convergence is considered to be reached when an error η has become sufficiently small (less than 1%). This error was evaluated by comparison with a reference solution $\mathbf{s_{ref}}$ obtained with the direct monolithic approach, see [21]. This reference solution was calculated using the same space and time discretizations as for the LATIN and ISPP methods: therefore, both algorithms converge toward this solution and the error η tends toward zero as the number of iterations increases. The evolution of the pore pressure in the domain as a function of time is shown in Fig. 22.

6.5.2 Illustration of the Use of the PGD Technique

Contrary to the case of weak fluid-structure coupling [27], classical staggered schemes, when applied to highly coupled problems such as fluid transfer in porous media, lack consistency [58, 79, 80]. The ISPP approach regains consistency thanks to the introduction of n_{sub} subcycles between the solid and the fluid solvers at each time step. Then, the

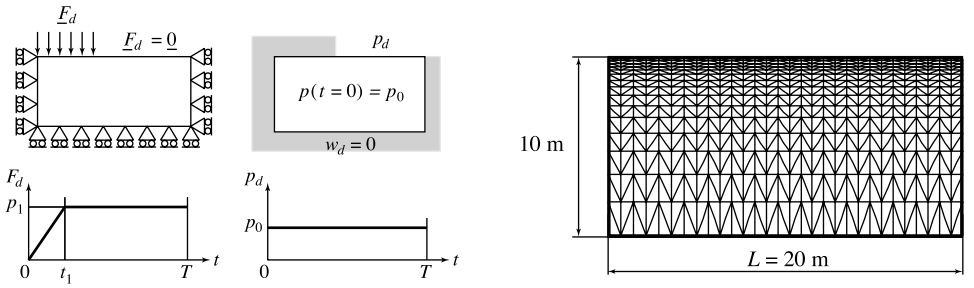

Fig. 21 Consolidation of a soil (*left*: prescribed solid quantities; *middle*: prescribed fluid quantities; *right*: time evolution of the loading)

Table 2 Poro-elastic material characteristics of a water-saturated Berea sandstone

Porosity	$n = 0.19$	Biot's modulus	$Q = 13.5$ GPa
Young's modulus	$E = 14.4$ GPa	Biot's coefficient	$b = 0.78$
Poisson's ratio	$\nu = 0.2$	Permeability	$\frac{K}{\mu_w} = 2\ 10^{-10}$ m^3 s kg^{-1}

number of global resolutions for each of the solid and the fluid solvers is $n_S = n_F = n_{sub} \times n_I$.

In the LATIN method without the PGD technique, two uncoupled problems are solved at each iteration and at each time step. If n_{iter} is the number of iterations required to reach convergence, the number of global resolutions is $n_S = n_F = n_{iter} \times n_I$ for each solver. With PGD, as shown in Algorithm 1, only few global resolutions (k_{max}) are necessary in each of the two physics to achieve the approximate solution at each iteration. In the case reported here, a criterion was set up in order to avoid generating new pairs when the use of the reduced basis was sufficient to improve the quality of the solution. This explains why the numbers of global resolutions n_S and n_F for the two physics can be different and can be less than the number of iterations n_{iter} of the method.

Table 3 summarizes the results obtained and shows that using the PGD technique to approximate the unknowns makes the LATIN method particularly advantageous in terms of computational efficiency because the number of global resolutions is drastically reduced.

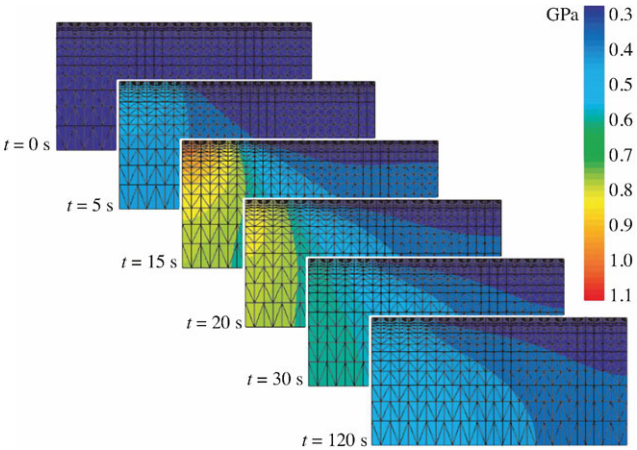

Fig. 22 Evolution of the pore pressure p as a function of time

Table 3 Number of global resolutions for the consolidation problem with $n_I = 120$

ISPP	$n_S + n_F$	1,080 + 1,080
	n_{sub}	9
LATIN without PGD	$n_S + n_F$	2,160 + 2,160
	n_{iter}	18
LATIN with PGD	$n_S + n_F$	8 + 16
	n_{iter}	27

7 Conclusion

In this paper, we presented a review of the use of Proper Generalized Decomposition in the framework of the LATIN method. The LATIN method was first described in detail in the case of a nonlinear evolution problem. Then, it was extended to the case of domain decomposition in order to deal with multiscale problems which can involve very different wavelengths, both in space and in time. Finally, we presented the use of the LATIN method for the resolution of multiphysics problems, where it enables one to avoid the simultaneous treatment of the different coupled phenomena. In all the cases studied, the advantage of using PGD compared to the incremental treatment of an evolution equation was underlined. PGD enables very significant gains in terms of computation cost and storage, which makes it a very promising tool for future calculation strategies. A first improvement, currently in progress, will be the introduction of a new algebra, *i.e.* a general mathematical framework, in which all functions are described using the radial time-space approximation. The final development, also dedicated to quasi-static problems, will deal with the extension to large-displacement problems following the mathematical framework already proposed in [51].

References

1. Akel S, Nguyen QS (1989) Determination of the limit response in cyclic plasticity. In: Proceedings of 2nd international conference on computational plasticity. Barcelone, Spain, pp 639–650
2. Ammar A, Mokdad B, Chinesta F, Keunings R (2006) A new family of solvers for some classes of multidimensional partial differential equations encountered in kinetic theory modeling of complex fluids. J Non-Newton Fluid Mech 139(3):153–176
3. Ammar A, Mokdad B, Chinesta F, Keunings R (2007) A new family of solvers for some classes of multidimensional partial differential equations encountered in kinetic theory modeling of complex fluids: Part II: Transient simulation using space-time separated representations. J Non-Newton Fluid Mech 144(2–3):98–121
4. Beckert A (2000) Coupling fluid (CFD) and structural (FE) models using finite interpolation elements. Aerosp Sci Technol 47:13–22
5. Belytschko T, Smolinski P, Liu WK (1985) Stability of multi-time step partitioned integrators for first-order finite element systems. Comput Methods Appl Mech Eng 49(3):281–297
6. Blom FJ (1998) A monolithic fluid-structure interaction algorithm applied to the piston problem. Comput Methods Appl Mech Eng 167:369–391
7. Bottasso CL (2002) Multiscale temporal integration. Comput Methods Appl Mech Eng 191(25–26):2815–2830
8. Caignot A, Ladevèze P, Néron D, Durand J-F (2010) Virtual testing for the prediction of damping in joints. Eng Comput 27(5):621–644
9. Champaney L, Cognard J-Y, Ladevèze P (1999) Modular analysis of assemblages of three-dimensional structures with unilateral contact conditions. Comput Struct 73:249–266
10. Champaney L, Boucard P-A, Guinard S (2008) Adaptive multianalysis strategy for contact problems with friction: application to aerospace bolted joints. Comput Mech 42(2):305–316
11. Chatterjee A (2000) An introduction to the proper orthogonal decomposition. Curr Sci 78(7):808–817
12. Chinesta F, Ammar A, Lemarchand F, Beauchene P, Boust F (2008) Alleviating mesh constraints: Model reduction, parallel time integration and high resolution homogenization. Comput Methods Appl Mech Eng 197:400–413
13. Cognard J-Y, Ladevèze P (1993) A large time increment approach for cyclic plasticity. Int J Plast 9:114–157
14. Combescure A, Gravouil A (2002) A numerical scheme to couple subdomains with different time-steps for predominantly linear transient analysis. Comput Methods Appl Mech Eng 191:1129–1157
15. Comte F, Maitournam H, Burry P, Lan NTM (2006) A direct method for the solution of evolution problems. C R Mec 334(5):317–322
16. Coussy O (2004) Poromechanics. Wiley, New York
17. Cresta P, Allix O, Rey C, Guinard S (2007) Nonlinear localization strategies for domain decomposition methods in structural mechanics. Comput Methods Appl Mech Eng 196(8):1436–1446
18. Devries F, Dumontet F, Duvaut G, Léné F (1989) Homogenization and damage for composite structures. Int J Numer Methods Eng 27:285–298
19. Dureisseix D, Farhat C (2001) A numerically scalable domain decomposition method for the solution of frictionless contact problems. Int J Numer Methods Eng 50:2643–2666
20. Dureisseix D, Ladevèze P, Néron D, Schrefler BA (2003) A multitime-scale strategy for multiphysics problems: application to poroelasticity. Int J Multiscale Comput Eng 1(4):387–400
21. Dureisseix D, Ladevèze P, Schrefler BA (2003) A computational strategy for multiphysics problems—application to poroelasticity. Int J Numer Methods Eng 56(10):1489–1510
22. Farhat C, Chandesris M (2003) Time-decomposed parallel time-integrators: theory and feasibility studies for fluid, structure, and fluid-structure applications. Int J Numer Methods Eng 58:1397–1434
23. Farhat C, Lesoinne M (2000) Two efficient staggered algorithms for the serial and parallel solution of three-dimensional nonlinear transient aeroelastic problems. Comput Methods Appl Mech Eng 182:499–515
24. Farhat C, Lesoinne M, LeTallec P (1998) Load and motion transfer algorithms for fluid/structure interaction problems with non-matching discrete interfaces: Momentum and energy conservation, optimal discretization and application to aeroelasticity. Comput Methods Appl Mech Eng 157:95–114
25. Faucher V, Combescure A (2003) A time and space mortar method for coupling linear modal subdomains and non-linear subdomains in explicit structural dynamics. Comput Methods Appl Mech Eng 192:509–533
26. Felippa CA, Geers TL (1988) Partitioned analysis for coupled mechanical systems. Eng Comput 5:123–133
27. Felippa CA, Park KC (1980) Staggered transient analysis procedures for coupled mechanical systems: formulation. Comput Methods Appl Mech Eng 24:61–111
28. Felippa CA, Park KC, Farhat C (2001) Partitioned analysis of coupled mechanical systems. Comput Methods Appl Mech Eng 190:3247–3270
29. Feyel F (2003) A multilevel finite element (FE^2) to describe the response of highly non-linear structures using generalized continua. Comput Methods Appl Mech Eng 192:3233–3244
30. Fish J, Chen W (2001) Uniformly valid multiple spatial-temporal scale modeling for wave propagation in heterogeneous media. Mech Compos Mater Struct 8:81–99
31. Fish J, Shek K, Pandheeradi M, Shephard MS (1997) Computational plasticity for composite structures based on mathematical homogenization: Theory and practice. Comput Methods Appl Mech Eng 148:53–73
32. Golub GH, Loan CFV (1996) Matrix computations, 3rd edn. Johns Hopkins University Press, Baltimore
33. Gosselet P, Chiaruttini V, Rey C, Feyel F (2004) A monolithic strategy based on an hybrid domain decomposition method for multiphysic problems. Application to poroelasticity. Rev Eur Élém Finis 13(5/7):523–534
34. Gravouil A, Combescure A (2001) Multi-time-step explicit implicit method for non-linear structural dynamics. Int J Numer Methods Eng 50:199–225
35. Gravouil A, Combescure A (2003) Multi-time-step and two-scale domain decomposition method for non-linear structural dynamics. Int J Numer Methods Eng 58:1545–1569
36. Guennouni T (1988) On a computational method for cycling loading: the time homogenization. Math Model Numer Anal 22(3):417–455 (in French)
37. Guidault P, Allix O, Champaney L, Cornuault S (2008) A multiscale extended finite element method for crack propagation. Comput Methods Appl Mech Eng 197(5):381–399
38. Gunzburger MD, Peterson JS, Shadid JN (2007) Reduced-order modeling of time-dependent pdes with multiple parameters in the boundary data. Comput Methods Appl Mech Eng 196(4–6):1030–1047
39. Hibbitt, Karlson, Sorensen (eds) (1996) Abaqus/standard—user's manual, vol I, pp 6.4.2–2 and 6.6.1–4
40. Huet C (1990) Application of variational concepts to size effects in elastic heterogeneous bodies. J Mech Phys Solids 38(6):813–841
41. Hughes TJR (1995) Multiscale phenomena: Green's function, the Dirichlet-to-Neumann formulation, subgrid scale models, bubbles and the origin of stabilized methods. Comput Methods Appl Mech Eng 127:387–401
42. Jolliffe I (1986) Principal component analysis. Springer, New York

43. Karhunen K (1943) Uber lineare methoden für wahrscheinigkeitsrechnung. Ann Acad Sci Fenn Ser A1 Math Phys 37:3–79
44. Kouznetsova V, Geers M, Brekelmans W (2002) Multi-scale constitutive modelling of heterogeneous materials with a gradient-enhanced computational homogenization scheme. Int J Numer Methods Eng 54:1235–1260
45. Kunisch K, Xie L (2005) Pod-based feedback control of the burgers equation by solving the evolutionary HJB equation. Comput Math Appl 49(7–8):1113–1126
46. Ladevèze J (1985). Algorithmes adaptés aux calculs vectoriels et parallèles pour des méthodes de décomposition de domaines. In: Actes du troisième colloque tendances actuelles en calcul de structures. Pluralis, pp 893–907
47. Ladevèze P (1985) On a family of algorithms for structural mechanics. C R Acad Sci 300(2):41–44 (in French)
48. Ladevèze P (1989) The large time increment method for the analyse of structures with nonlinear constitutive relation described by internal variables. C R Acad Sci Paris 309(II):1095–1099
49. Ladevèze P (1991) New advances in the large time increment method. In: Ladevèze P, Zienkiewicz OC (eds) New advances in computational structural mechanics. Elsevier, Amsterdam, pp 3–21
50. Ladevèze P (1997). A computational technique for the integrals over the time-space domain in connection with the LATIN method. Technical Report 193, LMT-Cachan (in French)
51. Ladevèze P (1999) Nonlinear computational structural mechanics—new approaches and non-incremental methods of calculation. Springer, Berlin
52. Ladevèze P, Nouy A (2003) On a multiscale computational strategy with time and space homogenization for structural mechanics. Comput Methods Appl Mech Eng 192:3061–3087
53. Ladevèze P, Loiseau O, Dureisseix D (2001) A micro-macro and parallel computational strategy for highly heterogeneous structures. Int J Numer Methods Eng 52:121–138
54. Ladevèze P, Néron D, Gosselet P (2007) On a mixed and multiscale domain decomposition method. Comput Methods Appl Mech Eng 196:1526–1540
55. Ladevèze P, Néron D, Passieux J-C (2009) On multiscale computational mechanics with time-space homogenization. In: Fish J (ed) Multiscale methods—Bridging the scales in science and engineering, Chapter space time scale bridging methods. Oxford University Press, Oxford, pp 247–282
56. Ladevèze P, Passieux J-C, Néron D (2010) The LATIN multiscale computational method and the proper generalized decomposition. Comput Methods Appl Mech Eng 199:1287–1296
57. Lefik M, Schrefler B (2000) Modelling of nonstationary heat conduction problems in micro-periodic composites using homogenisation theory with corrective terms. Arch Mech 52(2):203–223
58. Lewis RW, Schrefler BA (1998) The finite element method in the static and dynamic deformation and consolidation of porous media, 2nd edn. Wiley, New York
59. Lewis RW, Schrefler BA, Simoni L (1991) Coupling versus uncoupling in soil consolidation. Int J Numer Anal Methods Geomech 15:533–548
60. Lieu T, Farhat C, Lesoinne A (2006) Reduced-order fluid/structure modeling of a complete aircraft configuration. Comput Methods Appl Mech Eng 195(41–43):5730–5742
61. Maday Y, Ronquist EM (2004) The reduced-basis element method: application to a thermal fin problem. SIAM J Sci Comput 26(1):240–258
62. Maman N, Farhat C (1995) Matching fluid and structure meshes for aeroelastic computations: a parallel approach. Comput Struct 54(4):779–785
63. Matteazzi R, Schrefler B, Vitaliani R (1996) Comparisons of partitioned solution procedures for transient coupled problems in sequential and parallel processing. In: Advances in computational structures technology. Civil-Comp Ltd, Edinburgh, pp 351–357
64. Matthies HG, Steindorf J (2003) Partitioned strong coupling algorithms for fluid-structure interaction. Comput Struct 81:805–812
65. Michler C, Hulshoff SJ, van Brummelen EH, de Borst R (2004) A monolithic approach to fluid-structure interaction. Comput Struct 33:839–848
66. Morand J-P, Ohayon R (1995) Fluid-structure interaction: applied numerical methods. Wiley, New York
67. Néron D, Dureisseix D (2008) A computational strategy for poroelastic problems with a time interface between coupled physics. Int J Numer Methods Eng 73(6):783–804
68. Néron D, Dureisseix D (2008) A computational strategy for thermo-poroelastic structures with a time-space interface coupling. Int J Numer Methods Eng 75(9):1053–1084
69. Néron D, Ladevèze P, Dureisseix D, Schrefler BA (2004) Accounting for nonlinear aspects in multiphysics problems: Application to poroelasticity. In: Lecture notes in computer science, vol 3039, pp 612–620
70. Nouy A (2007) A generalized spectral decomposition technique to solve a class of linear stochastic partial differential equations. Comput Methods Appl Mech Eng 196(45–48):4521–4537
71. Nouy A (2009) Recent developments in spectral stochastic methods for the numerical solution of stochastic partial differential equations. Arch Comput Methods Eng 16(3):251–285
72. Nouy A, Ladevèze P (2004) Multiscale computational strategy with time and space homogenization: a radial type approximation technique for solving micro problems. Int J Multiscale Comput Eng 170(2):557–574
73. Oden JT, Vemaganti K, Moës N (1999) Hierarchical modeling of heterogeneous solids. Comput Methods Appl Mech Eng 172:3–25
74. Piperno S, Farhat C, Larrouturou B (1995) Partitioned procedures for the transient solution of coupled aeroelastic problems. Part I: model problem, theory and two-dimensional application. Comput Methods Appl Mech Eng 124:79–112
75. Ryckelynck D (2005) A priori hyperreduction method: an adaptive approach. J Comput Phys 202:346–366
76. Ryckelynck D, Chinesta F, Cueto E, Ammar A (2006) On the a priori model reduction: Overview and recent developments. Arch Comput Methods Eng 13(1):91–128
77. Sanchez-Palencia E (1974) Comportement local et macroscopique d'un type de milieux physiques hétérogènes. Int J Eng Sci 12(4):331–351
78. Sanchez-Palencia E (1980) Non homogeneous media and vibration theory. Lect Notes Phys 127
79. Turska E, Schrefler BA (1993) On convergence conditions of partitioned solution procedures for consolidation problems. Comput Methods Appl Mech Eng 106:51–63
80. Turska E, Schrefler BA (1994) On consistency, stability and convergence of staggered solution procedures. Rend Mat Acc Lincei 9(5):265–271
81. Vermeer PA, Veruijt A (1981) An accuracy condition for consolidation by finite elements. Int J Numer Anal Methods Geomech 5:1–14
82. Violeau D, Ladeveze P, Lubineau G (2009) Micromodel-based simulations for laminated composites. Compos Sci Technol 69(9):1364–1371
83. Zohdi T, Wriggers P (2005) Introduction to computational micromechanics. Springer, Berlin
84. Zohdi T, Oden J, Rodin G (1996) Hierarchical modeling of heterogeneous bodies. Comput Methods Appl Mech Eng 138(1–4):273–298
85. Zohdi TI (2004) Modeling and simulation of a class of coupled modeling and simulation of a class of coupled thermo-chemo-mechanical processes in multiphase solids. Comput Methods Appl Mech Eng 193:679–699